Analysis of Peristaltic MHD Ellis Fluid in a Porous Inclined Asymmetric Channel

By

Aqib Javid Kayani

DEPARTMENT OF MATHEMATICS

NATIONAL UNIVERSITY OF MODERN LANGUAGES

ISLAMABAD,

May 2025

Analysis of Peristaltic MHD Ellis Fluid in a Porous Inclined Asymmetric Channel

by

AQIB JAVID KAYANI

Supervised by

Dr. Hadia Tariq

MS Mathematics, National University of Modern Languages, Islamabad

A THESIS IS SUBMITTED IN PARTIAL FULFILLMENT OF
THE REQUIREMENT OF DEGREE OF

MASTER OF SCIENCE

IN MATHEMATICS

TO
FACULTY OF ENGINEERING AND COMPUTING

NATIONAL UNIVERSITY OF MODERN LANGUAGES ISLAMABAD

THESIS AND APPROVAL FROM

The undersigned certify that they have read the following thesis, examined the defense, are satisfied with overall exam performance, and recommend the thesis to the Faculty Engineering and Computing for acceptance.

Thesis Title: Analysis of Peristaltic MHD Ellis Fluid in a Porous Inclined Asymmetric Channel

Submitted By: Aqib Javid Kayani **Registration:**78 MS/Math/S23

Master of Science in Mathematics (MS Math)
Title of the Degree

Mathematics
Name of Discipline

Dr. Hadia Tariq _____
Name of Research Supervisor Signature of Research Supervisor

Dr. Sadia Riaz _____
Name of HOD (Math) Signature of HOD (Math)

Dr. Noman Malik _____
Name of Dean (FEC) Signature of Dean (FEC)

AUTHOR'S DECLARATION

I Aqib Javid Kayani

Son of Muhammad Javid Kayani

Registration # 78 MS/Math/S23

Discipline Mathematics

Candidate of **Master of Science in Mathematics (MS Math)** at the National University of Modern Languages do hereby declare that the thesis**: Analysis of peristaltic MHD Ellis fluid in a porous inclined asymmetric channel** submitted by me in partial fulfillment of MS Mathematics degree, is my original work, and has not been submitted or published earlier. I also solemnly declare that it shall not be submitted by me for obtaining any other degree from this or any other university or institution in the future. I also understand that if evidence of plagiarism is found in my thesis/dissertation at any stage, even after the award of a degree, the work may be cancelled and the degree revoked.

Signature of Candidate

Aqib Javid Kayani

Name of Candidate

Date . 29 May, 2025

ABSTRACT

Title: Analysis of Peristaltic MHD Ellis Fluid in a Porous Inclined Asymmetric Channel

This thesis aims to investigate the effects of heat and mass transfer on the peristaltic flow and investigate the peristaltic transport of Ellis fluid in a porous inclined asymmetric channel. The study also considers slip conditions. The governing equations for Ellis fluid are introduced. Stream functions are taken into account to reduce the number of dependent variables in the governing PDEs. These equations are then solved using the perturbation method to provide temperature and velocity profiles. The impact of various parameters on temperature, pressure, velocity, and streamlines is examined. The graphs were generated using the Mathematica software.

TABLE OF CONTENTS

CHAPTER	TITLE	PAGE
AUTHOR'S DECLARATION		iv
ABSTRACT		v
TABLE OF CONTENTS		vi
LIST OF FIGURES		ix
LIST OF SYMBOLS		x
ACKNOWLEDGMENT		xi
1	**INTRODUCTION AND LITERATURE REVIEW**	**1**
1.1 Introduction		1
1.2 Peristalsis		1
1.3 Magnetohydrodynamics		2
1.4 Ellis Fluid Model		3
1.5 Porous Medium		4
1.6 Heat Transfer		5
1.7 Asymmetric Channel		6
1.8 Contribution to Thesis		7
1.9 Thesis Organization		7
2	**BASIC DEFINATIONS AND CONCEPTS**	**9**
2.1 Dynamics of Fluid		9
2.2 Fluid		9
2.2.1 Newtonian Fluid		10
2.2.2 Non-Newtonian Fluid		10
2.2.3 Ideal Fluid		11

2.2.4 Real Fluid 11

2.2.5 Compressible Fluid 11

2.2.6 Incompressible Fluid 12

2.2.7 Laminar Flow 12

2.2.8 Turbulent Flow 12

2.3 Density 12

2.4 Ellis Fluid 13

2.5 Streamlines 14

2.6 Stress 14

2.7 Cauchy Stress Tensor 14

2.8 Extra Stress Tensor 15

2.9 Specific Heat Capacity 15

2.10 Pressure 15

2.11 Thermal Conductivity 15

2.12 Newton's Law of Viscosity 16

2.13 Viscosity 16

2.14 Heat Transfer 16

2.14.1 Conduction 17

2.14 .2 Convection 17

2.14.3 Radiation 17

2.15 Non-dimensional Parameter 17

2.15.1 Prandtl Number 17

2.15.2 Eckert Number 18

2.15.3 Brinkman Number 18

2.15.4 Schmidt Number 19

2.16 Equation of Continuity 19

2.17 Momentum Equation 19
2.18 Energy Equation 20
2.19 Perturbation Method 20
2.20 Heat Flux 21
2.21 Velocity Field 21
2.22 Lubrication Approach Theory 21

3 THE PERISTALTIC FLOW OF CHEMICALLY REACTIVE ELLIS FLUID THROUGH AN ASYMMETRIC CHANNEL HEAT AND MASS TRANSFER ANALYSIS 22

3.1 Introduction 22
3.2 Mathematical formulation 22
3.3 Exact solution 26
3.4 Results & Discussions 28
3.5 Conclusion 29

4 ANALYSIS OF PERISTALTIC MHD ELLIS IN POROUS INCLINED ASYMMETRIC CHANNEL 35

4.1 Introduction 35
4.2 Problem formulation 35
4.3 Results & Discussion 39

5 CONCLUSION AND FUTURE WORK 48

References 50

LIST OF FIGURES

FIGURE NO	TITLE	PAGE
3.1	Variation of α on velocity profile	30
3.2	Variation of β on velocity profile	30
3.3	Impact of phase angle $\emptyset$ on velocity profile	31
3.4	Graphical Illustration of Δp with diverse values of α	31
3.5	Graphical Illustration of Δp with diverse values of β	32
3.6	Graphical Illustration of temperature θ with diverse values for α	32
3.7	Graphical Illustration of temperature with diverse values of β	33
3.8	Graphical Illustration of Concentration with diverse values of β	33
3.9	Graphical Illustration of Concentration with diverse values of γ	34
3.10	Graphical Illustration of Concentration with diverse values of Sc.	34
4.1	Visual Framework of the Proposed Channel.	35
4.2	Influence of β on velocity profile	40
4.3	Effect of porosity k_1 on velocity profile	41
4.4	Effect of α on the velocity field	41
4.5	Effect of Magnetic Parameter M on the velocity field	42
4.6	Variation of pressure gradient under the influence of α	42
4.7	Graphical portrayal of pressure gradient for the values of M	43
4.8	The variation of pressure gradient under the influence of β	43
4.9	The effect of porosity k_1 on the pressure gradient	44
4.10	Effect pressure gradient under the influence of Fr	44
4.11	Graphical portrayal of pressure gradient under the influence of γ	45
4.12	The variation of temperature under the influence of M	45
4.13	The change of temperature for β	46
4.14	Graphical portrayal of temperature under the influence of k_1	46
4.15	Effect of α on temperature θ	47
4.16	Graphical portrayal of temperature under the influence of Br	47

LIST OF SYMBOLS

ρ	Density
P	pressure
μ	viscosity
b	Amplitude
c	Wave speed
λ	Wavelength
B_o	Magnetic field
n	Dimensional parameter
Ψ	Stream function
u	velocity in x-direction
v	velocity in y-direction
Re	Reynold number
α	Inclination of the channel
Ec	Eckert number
k_1	Porosity
δ	wave number
β	Ellis Fluid Parameter

ACKNOWLEDGMENT

I want to thank Allah almighty for making this study possible and fruitful. Without the sincere support provided by numerous sources for which I would want sincerely thank you this project could not have been completed. I owe a debt of gratitude to Dr. Hadia Tariq whose counsel, insight and steadfast support have been invaluable to me during study process. I consider myself extremely formulate to have had you as my mentor because your knowledge and guidance have been helpful.

CHAPTER NO 1

INTRODCTION AND LITERATURE RIVEW

1.1 Introduction

Fluid mechanics states that a fluid can be recognized by its behavior under external forces. When a solid is sheared, it deforms until the tension applied from the outside equals the internal shear resistance. A fluid is a substance that tends to flow. A fluid substance can generally spread and change shape in response to its environment without providing internal resistance. A substance is fluid if it has a definite structure and can yield easily to external pressure. Fluid mechanics provides the framework for comprehending the behavior of fluids both at rest and in motion. It provides knowledge of fluid behavior, energy conservation, and system design in a range of real-world scenarios, making it essential to the natural sciences and engineering.

1.2 Peristalsis

The periodic contractions of the muscles lining tubular organs, including the gastrointestinal tract, are referred as peristalsis. This procedure makes it easier for substances to pass through these organs, which helps with waste removal, nutrition absorption, and digestion. The autonomic nervous system controls peristalsis, an involuntary mechanism that facilitates the smooth transfer of materials and food from the mouth to the anus. Latham [1] was the first to describe and investigate the peristaltic process. Shapiro *et al.* [2] enhanced Latham's notion by assuming peristaltic pumping in a 2-D channel with a long wavelength assumption. By taking into account the higher-order components and expanding the research to include scenarios with greater

Reynolds numbers intended by Shapiro [2], Jaffrin [3] improved the low Reynolds number hypothesis that was initially proposed.

Mishra and Rao [4] provided an explanation of the peristaltic phenomena in viscous fluid flow in an asymmetrical channel, as well as the high wavelength and minimal Reynolds number assumptions. Srivastasa *et al*. [5] studied blood peristaltic transport using the Casson model, highlighting the non-Newtonian nature of most natural fluids, impacting both physical and scientific aspects. Nadeem and Akbar [6] examined the peristaltic flows of Williamson fluids along an inclined, asymmetrical channel utilizing partial slip and heat transmission effects. Abd El Hakeem *et al*. [7] investigated peristaltic viscous flow in an endoscope use and found that pressure increased with wave number, amplitude, and radius ratio but decreased with viscosity ratio. Burns and Parkes [8] investigated creeping flow in the framework of peristaltic flow across vertically symmetrical pipes and channels. Vaidya *et al*. [9] examined how several parameters affected the Jeffrey fluid flow through an asymmetric tapering permeable channel exhibiting the peristaltic mechanism.

Ali and Hayat [10] analyzed the micropolar fluid in an asymmetrical conduit with peristaltic waves induced at the walls. Nadeem *et al*. [11] investigated the effects of magnetic fields and viscosity on the peristaltic flow of a viscous, incompressible Newtonian fluid. The perturbation expansion approach produces analytical solutions to both temperature and fluid velocity. Using common perturbation expansion techniques, the temperature and velocity fields' analytical solutions are obtained.

1.3 Magnetohydrodynamics

Magnetohydrodynamics is the investigation of magnetic field dynamics in electrically conducting fluids. It combines concepts from magnetism and fluid dynamics. Hannes Alfvan is credited with developing the field of MHD [12]. In 1970, he was also awarded a Nobel Prize. Fluid dynamics uses the Naiver-Stokes equations to describe MHD, whereas electromagnetics uses the Maxwell equations to illustrate MHD. Gnaneswara and Venugopal [13] investigated the influence of joule heating and chemical reactions on MHD peristaltic flow in a porous media. Rafiq *et al*.

[14] investigated the impact of activation energy, magnetohydrodynamics and variable characteristics of the peristaltic flow of Jeffrey fluid in a porous wall channel.

Gnaneswara *et al*. [15] described MHD peristaltic flow in a pair stress fluid along an asymmetric porous channel. Long wavelength and low Reynolds number assumptions were used in the non-dimensional governing flow equations. Abbasi *et al*. [16] studied the MHD peristaltic transport of nanofluids. The investigation used temperature and velocity slip conditions, as well as four distinct types of nanoparticles: gold, copper, silver, and iron oxide. Ali *et al*. [17] studied the peristaltically accelerated MHD Jeffrey nanofluids' flow and slip characteristics. The study explores Jeffrey Nanofluids' peristaltic flow within a magnetic field, aiming to understand how nanofluids transport heat for potential cancer treatment. Srinivas and Kothandapani [18] examined MHD peristaltic flow in a porosity zone with compliant walls to explore the effects of heat and mass transmission.

1.4 Ellis Fluid Model

One particular type of non-Newtonian fluid model used to explain the rheological properties of particular fluids is the Ellis fluid model. Newtonian fluids have a viscosity that fluctuates with the shear rate, whereas Newtonian fluids have a viscosity that remains constant independent of the applied shear rate. The Ellis model predicts the behavior of materials under various flow circumstances, which aids in the design of machinery and procedures for the production of paints, polymers, and other shear-thinning materials.

An Ellis model subclass is a generalized Newtonian fluid with low shear forces due to shear thinning, indicating Newtonian behavior without shear pressures. Ellis fluid bioconvective flow was numerically simulated by Ahmed *et al.* [19]. The finite difference technique was used to build the mathematical algorithm for nanofluid flow that takes into consideration of the activation energy distribution throughout the wedge. Saravana *et al*. [20] evaluated the impact of total velocity slip on the axisymmetric peristaltic transfer of Ellis fluid through a uniformly flexible tube using a long wavelength and a very low Reynold number.

Goud and Reddy [21] used long wavelengths and imprecise estimates of the Reynolds number to explain the Ellis fluid model traveled in a uniform upward tube across wall defects. Ellis fluid viscoelastic characteristics were examined by Asghar *et al*. [22] centered on chemical reactions, wave propagation, and the connection between magnetic fields and slip conditions. Narahari *et al*. [23] examined the peristaltic flow of an Ellis fluid through a circular tube. Abbas *et al.* [24] demonstrated the peristaltic flow of Ellis fluid in a non-uniform conduit with compliant walls. For the Ellis model, Khan *et al*. [25] used hybrid nanoparticles to investigate the effects of both consistent and different conditions on the creation of entropy analysis. Kumar *et al*. [26] investigated the peristaltic pumping of an Ellis fluid model in an inclined tube with wall properties.

1.5 Porous Medium

A substance having pores is called a porous medium. Generally, a fluid (gas or liquid) fills the pores. Porous voids can be observed in many natural and artificial systems, including tissues from living organisms, rocks, soil, and man-made materials like ceramics, foams, and sponges. Porous media are crucial for numerous industrial uses as well as natural processes.

El Shehawey and Husseny [27] proposed a mathematical model for the peristaltic movement of an incompressible, viscous fluid across a porous medium. The study investigated peristaltic pumping in a porous channel filled with viscous, incompressible fluid, revealing nonsymmetric fluid motion, increasing mean axial velocity, and reversal flow with varying permeability parameters. El-Sayed *et al*. [28] explored how the mass distribution of chemical species affected heat transfer across vertical porous media and peristaltic transport between circular tubes with mass. The effects of vacuum porosity and heat transfer on a peristaltic movement in a vertical asymmetry channel were studied by Mekheimer *et al.* [29]. The perturbation approach was used to solve the nonlinear PDE system after the governing equations were linearized using the long wavelength approximation. Frictional forces and pressure rise were computed numerically yet the flow is analyzed. Using the homotopy perturbation method, Tripathi and Bég [30] examined a modified Maxwell fluid's peristaltic flow through a porous media.

The Hall effect and the peristaltic flow of a Maxwell fluid through a porous medium were examined by Hayat *et al.* [31]. Vajravelu *et al.* [32] examined heat transmission and peristalsis in flow through a vertical porous tube. Bhargava *et al.* [33] demonstrated the peristaltic flow of blood through stenosed arteries by treating arteries as porous channels and blood as a micro-polar fluid. Hayat *et al*. [34] investigated the peristaltic motion of an electrically conducting fluid with heat transfer across a porous area.

1.6 Heat Transfer

Heat transfer processes can be broadly classified into three categories: radiation, convection, and conduction. Nadeem and Akbar [35] investigated the impact of heat and mass transfer on peristaltic motion across an annulus with a radically changing magnetic field. Ellahi *et al.* [36] examined the three-dimensional peristaltic flow with mass and heat transfer through a non-uniform rectangular conduit and obtained precise solutions. Ogulu [37] investigated blood mass and heat transfer in a single lymphatic artery with a consistent magnetic field. The cumulative impact of concentration and heat convection on the peristaltic Powell-Eyring nanofluid transport in an inclined asymmetrical channel was examined by Akram *et al.* [38].

The impact of heat and mass transfer on the peristaltic transport of Maxwell fluid with creeping flow was theoretically examined by Saleem and Haider [39]. The study of mixed convective heat and mass transfer on peristaltic flow of Fene-P fluid with chemical reaction was investigated by Asghar and Ali [40]. A vertical tube's magnetohydrodynamic peristaltic flow of Jeffery nanofluid with heat transfer across a porous media was examined by Eldabe *et al.* [41]. A comprehensive investigation of peristaltic flow in connection to Prandtl material properties and heat transmission was presented by Alsaedi *et al.* [42].

Tamizharasi *et al.* [43] investigated the heat and mass transport phenomenon in the peristalsis of nanoliquid utilizing an asymmetric arrangement of infinite length. Hina *et al.* [44] used the Buongiorno mode to investigate the peristaltic movement of the asymmetric channel carrying a Carreau-Yasuda nanofluid. A Buongiorno model was adopted with electro-kinetic body force and

a Carreau-Yasuda nanofluid, the work investigated peristaltic flow in an asymmetric channel. The Debye-Huckel linearization assumption and the lubrication approximation were applied. Using a temperature-dependent viscosity effect, Hasona *et al.* [45] measured the peristaltic movement's heat transfer of Jeffrey the nanofluid by analyzing the fluid's physical characteristics.

1.7 Asymmetric Channel

A flow path where the geometry or boundary conditions are not symmetric concerning the centerline is referred to as an asymmetric channel. These channels are frequently seen in natural systems and a variety of technical applications where a non-uniform flow field is produced by the form, boundary conditions, or other reasons. Because of their irregular form, asymmetric channels can display diverse flow characteristics and behaviors.

To evaluate the significance of the heat transference study of an MHD peristaltic flow, an asymmetric permeability channel with slipping conditions and fluid dissipation components was investigated by Das [46]. A Jeffrey fluid's peristaltic flow in an asymmetrical channel was investigated by Abd-Alla *et al.* [47]. Shear stress, axial velocity, stream operation, pressure gradient, and pressure rise on the channel walls were all numerically calculated using closed-form formulas based on long wavelength and Low Reynolds number assumptions.

The MHD peristaltic flow of a viscous fluid in an asymmetry channel with heat transfer has been investigated by Srinivas and Kothandapani [48]. The MHD peristaltic motion of a Sisko fluid in an asymmetric channel was analyzed by Wang *et al.* [49]. Abd-Alla *et al.* [50] investigated a fluid that was peristaltically moving in an asymmetric, inclined channel. A mathematical analysis of the peristaltic flow of blood along an inclined asymmetric channel with mass transfer, heat and an inclined magnetic field was done.

Elshehawey *et al.* [51] examined the problem of peristaltic movement of a viscous incompressible in an asymmetric channel. Using the Adomian decomposition approach, they were able to provide

an explicit description of the peristaltic passage across fluid with holes in asymmetric channels. The study examined the impact of low Reynolds number assumption and longer wavelength on pressure rise, velocity field, and pumping characteristics.

Javed *et al*. [52] investigated the impact of porosity on biological flow in curved channels. They concluded that sinusoidal waves enhance porosity effects, which increases efficacy and creates new bioengineering opportunities for mediation systems and chemical processes.

1.8 Contribution to Thesis

This thesis includes a detailed analysis of Abbasi's work [55]. This research work is extended by taking inclined asymmetric passage along with magnetic field also inclined and porosity. The temperature profile of the model is also examined and graphs for the velocity, pressure gradient and temperature are plotted to check the impact of the added body forces on the model.

1.9 Thesis Organization

Chapter 1 provides a few basic definitions related to the proposed work. A brief literature survey is also included in each section to build a base of the suggested model.

Chapter 2 offers basic concepts and dimensional parameters that are utilized to get the results of flow patterns.

Chapter 3 presents a comprehensive review of the peristaltic flow of a chemically reactive Ellis fluid through an asymmetric channel, focusing on the analysis of heat and mass transfer. This research was done by Abbasi *et al.* [55].

Chapter 4 delivers a detailed extended model of the work discussed in Chapter 3. Graphical demonstration of the velocity, pressure gradient and temperature profiles of the fluid are also included to check the impact of inclined magnetic field parameter, porosity parameter, Ellis fluid parameter and others.

Chapter 5 contains the conclusions derived in chapter 4. This chapter also offers how this proposed model can be extended.

All references used in this study are provided at the end of the document.

CHAPTER NO 2

BASIC DEFINITIONS AND CONCEPTS

This chapter includes basic definitions and guidelines to help readers comprehend the analysis.

2.1 Dynamics of Fluid

The mechanics of fluids is a branch of physics that studies the properties of gases, liquids, and plasmas in both static and moving states. It covers two primary topics: fluid dynamics, which deals with fluids in motion, and fluid statics, which studies fluids that are not moving. Important ideas like pressure, flow rate, and viscosity which characterize how fluids behave under various stresses and conditions are explored in this discipline. Understanding how water flows through pipes, how air moves around airplanes, and even how blood circulates in the human body are just a few of the many uses for fluid mechanics. Since it is fundamental to understanding the behavior of liquids and gases, fluid mechanics is used extensively in many fields. For example, in civil engineering, it helps with the design of water supply systems, dams, and flood control structures; in mechanical engineering, it optimizes hydraulic systems, HVAC systems, and refrigeration processes; in the aerospace industry, fluid mechanics is used to understand aerodynamics, which is important for designing aircraft and spacecraft; in automotive engineering, it enhances vehicle fuel efficiency and aerodynamics; and in environmental engineering, it is used to control water flow, wastewater treatment, and pollution control.

2.2 Fluid

Any substance that rapidly flows and changes shape in response to an applied force is considered a fluid. Gases, plasmas, and liquids are examples of fluids. Fluids assume the shape of their container and lack a distinct shape, in contrast to solids, which have a set shape. A substance is said to be fluid if it has a definite structure and can yield easily to external pressure. Fluids are materials that have zero shear modulus, meaning that they are unable to withstand shear forces, [53]. Fluids can be broadly classified into numerous types based on their physical attributes and actions. Here are a few common types of fluids:

2.2.1 Newtonian Fluid

Shear stress and deformation rate in Newtonian fluids, which are capable of having unchanging viscosities, are directly and linearly correlated. In fluids where particle contact has no effect on flow behavior, Newtonian behavior is observed. Among them are water, air, and most oils, [53].

2.2.2 Non-Newtonian Fluid

Depending on conditions, non-Newtonian fluids show a relationship that is not linear between stress and deformation rate as well as variable viscosity. Another name for these fluids is second-grade fluids. Different circumstances cause these fluids to behave differently when they flow. Ketchup and toothpaste are two examples. Based on their viscosity, non-Newtonian fluids are further separated into Bingham and pseudo-plastic fluids, [53].

- Shear-Thinning Substances
  Viscosity falls as the shear rate rises. (such as blood or ketchup)

- Shear-Thickening Fluids

As the shear rate increases, viscosity increases. (Examples are water and cornstarch mixture).

- Viscoelastic Fluids

Exhibit both flexible and viscoelastic properties (Examples are Silly Putty, polymer solutions).

2.2.3 Ideal Fluid

Ideal fluids are a theoretical concept. Perfect fluids are said to have possess constant density and incompressibility and lack turbulence, surface tension, and viscosity. Perfect fluids sustain constant pressure over time, [53].

2.2.4 Real Fluid

Real fluids behave differently from ideal ones because of their viscosity, compressibility, and other characteristics. Oils, air, and water are a few examples, [53].

2.2.5 Compressible Fluid

These fluids' volume and density can change in response to changes in pressure and temperature. These liquids behave in a manner akin to gasses. When there is a sudden shift in pressure, these fluids can produce shock waves. (e.g. air, hydrogen), [53].

2.2.6 Incompressible Fluid

These fluids have a constant volume regardless of changes in temperature and pressure. These materials behave like liquids. Incompressible fluids are heat transfer mediums because their fixed volume features provide consistent heat exchange performance. (e.g. water, oil), [48].

2.2.7 Laminar Flow

This type of fluid flow is distinguished by the fluid flowing in parallel, smooth layers with minimal disruption between them. Laminar flow produces a continuous and predictable motion by having adjacent fluid layers slide past one another in an ordered manner. The fluid moves at a relatively slow speed, with viscous forces outweighing inertial forces, [53].

2.2.8 Turbulent Flow

Turbulent flow is defined by disorganized, irregular fluid motion where the fluid particles travel in a disorderly and unpredictable manner. Eddies and swirls are produced in turbulent flow, which causes a substantial amount of mixing between the fluid layers. This kind of flow happens quickly and is primarily driven by inertial forces as opposed to viscous forces, [53].

2.3 Density

The quantity of mass that a substance contains in a specific volume is measured by its density. In mathematical terms, it is stated as

$$\rho = \frac{mass}{volume}.$$

Density is measured in kilograms per cubic meter (kg/m3), The International System of Units' standard unit of density (SI). On smaller scales, density can alternatively be expressed in per cubic centimeter, in grams (g/cm^3) and its dimension is [ML^{-3}],[54].

2.4 Ellis Fluid

When the force applied to an Ellis fluid increases, its viscosity lowers, making it a non-Newtonian shear-thinning fluid whose viscosity rises as shear force increases. The Ellis fluid model is specifically intended to explain the flow properties of fluids that, while exhibiting non-Newtonian features (shear-thinning) at higher shear stress, behave like Newtonian fluids at low shear stress.

A structural model called the Ellis fluid model is used to explain the flow characteristics of several non-Newtonian fluids, particularly shear-thinning fluids. This model describes fluids whose viscosity reduces with increasing applied shear stress. Compared to more straightforward models like the power-law model, it offers a more accurate estimate of viscosity behavior at both low and high shear rates.

The Ellis fluid Model equation is

$$\frac{\mu}{\mu_1} = 1 + \left(\frac{\tau}{\tau_1}\right)^{\alpha-1}.$$

The viscosity at a given symbol for shear stress is μ, the zero shear viscosity is represented by μ_1 and the viscosity at very low Shear stress is generated by τ , the shear stress at which the viscosity is decreased to half of the viscosity at zero shear and the dimensionless parameter α controls how much shear-thinning there is.

2.5 Streamline

A line is drawn in a fluid flow field so that, at any given position, the fluid's velocity is perpendicular to the line. Streamlines describe the instantaneous direction of fluid motion in stable flows. A streamline is a path that depicts the steady-flowing flow of a fluid, such as water or air. The fluid's velocity vector, which indicates the direction of the fluid's motion at each point along a streamline, is tangent to the line at that location, [54].

2.6 Stress

The internal force per unit area that a material creates in reaction to an externally applied force is called stress. It shows how strong internal forces are within a material to prevent deformation in response to loads from the outside.

Stress can be expressed mathematically as:

$$\sigma = \frac{F}{A}.$$

In the SI, the Pascal (Pa), which is equivalent to one Newton per square meter Nm^2, is the unit of stress.

2.7 Cauchy Stress Tensor

Cauchy stress tensors describe the internal forces that are dispersed throughout a fluid as a result of external loads, pressure, and other reasons. It characterizes the level of stress in a fluid at a specific place. It is essential to comprehend how fluids behave mechanically under different flow circumstances, [54].

2.8 Extra Stress Tensor

Analyzing viscous behavior in fluids requires an understanding of the link between the rate of strain tensor and the extra stress tensor in fluid mechanics. In Newtonian fluids, where the rate of strain tensor through the dynamic viscosity is precisely proportional to the additional stress tensor, this relationship is very important, [54].

2.9 Specific Heat Capacity

Specific heat capacity, or simply specific heat, is the amount of heat needed to raise a substance's temperature by one degree Celsius (or one Kelvin) per unit mass. It is an essential characteristic of fluid mechanics and thermodynamics because it affects the fluid's response to heat transfer, [54].

2.10 Pressure

According to fluid mechanics, pressure (P) is the normal force that a fluid at rest or in motion exerts per unit area. It demonstrates the force that fluid molecules apply when they interact with a surface.

Mathematically

$$P = \frac{F}{A}.$$

Pressure is measured in Nm^{-2} its dimension is $[ML^{-1}T^{-2}]$.

2.11 Thermal Conductivity

The characteristic that reflects a material's capacity to conduct heat is called thermal conductivity. It measures the speed at which a temperature differential causes heat to move through a substance.

Fourier's law of heat conduction, which asserts the following, is frequently used to express the thermal conductivity (*k*):

$$q = -KA\frac{\Delta T}{L},$$

thermal conductivity is measured in watts per meter-kelvin ($WM^{-1}K^{-1}$) in SI units.

2.12 Newton's Law of Viscosity

According to the law of viscosity by Newton, the rate of shear stress is exactly proportional to shear strain in a fluid.

Its formula is given by

$$\tau = \mu\frac{du}{dy}.$$

2.13 Viscosity

A fluid's resistance to flow or deformation is measured by its viscosity. It indicates how "thick" or "sticky" a fluid is, to put it another way. Internal friction, which occurs when fluid molecules move relative to one another, is the cause of viscosity. A fluid's resistance to flow and deformation is measured by its viscosity. Viscosity is a measure of a fluid's thickness or stickiness; a higher viscosity indicates more internal friction between fluid molecules.

2.14 Heat Transfer

The movement of thermal energy from one physical system to another as a result of a temperature differential is known as heat transfer. The flow of energy is always from a hotter region to a colder region until thermal equilibrium is achieved.

The transfer of heat occurs primarily in three ways.

2.14.1 Conduction

This occurs when heat is transferred through a substance without the substance moving at all. It happens when energy is transferred from molecules or atoms to one another through vibrations and collisions. For example, when one end of a metal rod is heated, heat flows through it.

2.14.2 Convection

In this instance, heat is transferred from a solid surface to a moving fluid, like a gas or liquid. The combined effects of fluid motion, which improves heat transfer, and conduction (inside the fluid) result in convection.
Heat transmission from a heated surface to air passing over it is one example.

2.14.3 Radiation

Radiation specifically, is one type of electromagnetic wave that is used in this manner of heat transmission. Heat transmission can happen in a vacuum and doesn't need a medium.
Heat transmission from the Sun to the Earth, for instance.

2.15 Non-Dimensional Parameters

2.15.1 Prandtl Number

A dimensionless quantity called the Prandtl number (P_r) is used in heat transfer and fluid mechanics to describe the relative thickness of a fluid's thermal and velocity boundary layers. It

gives an indication of how important thermal diffusivity, or heat conduction, is compared to momentum diffusivity, or viscous effects, in a fluid flow.

The kinematic viscosity to The Prandtl number is the ratio of dispersion to heat.

$$Pr = \frac{\mathrm{v}}{\alpha^*}.$$

The fluid's kinematic viscosity (m^2/s) is denoted by ν, while its thermal diffusivity (m^2/s) is represented by α^*.

As an alternative, it might be stated as:

$$Pr = \frac{\mu c_p}{k}.$$

2.15.2 Eckert Number

The dimensionless Eckert number (Ec), which is used in fluid mechanics and heat transfer, shows the association between kinetic energy and enthalpy in a flow. It is the ratio of the flow's kinetic energy to the enthalpy difference caused by fluctuations in temperature.

The Eckert number formula is as follows:

$$Ec = \frac{u^2}{Cp\Delta T}.$$

.

2.15.3 Brinkman Number

The importance of viscous dissipation the transformation of mechanical energy into heat as a result of viscosity in relation to conductive heat transmission in a fluid flow is gauged by the dimensionless Brinkman number (Br). It is particularly helpful in situations with high-viscosity fluids or significant frictional heating, like in high-viscosity materials, high-speed flows, or lubrication.

$$Br = \frac{\mu C^2}{K\Delta T}.$$

The fluid's dynamic viscosity ($Pa.s$) is represented by μ, its characteristic velocity (m/s) by u, its conductivity of heat by k, and the temperature differential (K) by ΔT.

2.15.4 Schmidt Number

Schmidt number (Sc) is a dimensionless quantity in fluid dynamics and mass transfer processes. It is employed to characterize fluid flows in which mass diffusion and momentum processes occur simultaneously. It is the mass diffusivity divided by momentum diffusivity (kinematic viscosity).

$$Sc = \frac{\mu}{D}.$$

2.15.5 Froude Number

Froude number (Fr) is a dimensionless quantity in fluid dynamics. It is the ratio of inertial force to the gravitational force. It helps to classify the different flow regimes (fluvial or torrential motion).

2.16 Equation of Continuity

A fundamental concept in fluid mechanics, the equation of continuity describes how mass is conserved in a fluid flow. It asserts that, under steady flow and no mass buildup, a fluid's mass flow rate must stay constant across a pipe or channel's cross sections.

The continuity equation's differential form for a typical three-dimensional compressible fluid flow is:

$$\frac{\partial \rho}{\partial t} + \boldsymbol{\nabla}.(\rho \boldsymbol{V}) = 0.$$

.

The divergence operator is indicated by the symbols ∇, ρ is the fluid density (kg/m^3), Velocity ($\mathrm{m/s}$) is represented by $\boldsymbol{V}$, and time by t.

2.17 Momentum Equation

The conservation of momentum, which postulates that the sum of the external forces acting on a fluid element equals the rate at which its momentum changes, is expressed mathematically by the momentum equation in fluid mechanics. It describes the behavior of fluids under external body force, pressure, and viscosity. It comes from Newton's second law of motion. The general momentum equation, for an incompressible fluid is

$$\rho\left(\frac{\partial \boldsymbol{V}}{\partial t} + \boldsymbol{V}.\nabla\boldsymbol{V}\right) = -\boldsymbol{\nabla}.\boldsymbol{\tau} + \rho\boldsymbol{b}.$$

.

The fluid density is denoted by ρ, the velocity vector by $\boldsymbol{V}$, the time by t, $\boldsymbol{\tau}$ signifies Cauchy stress tensor while the body forces are represented by $\boldsymbol{b}$.

2.18 Energy Equation

The First Law of Thermodynamics, also referred to as the Law of Energy Conservation is frequently used to develop the energy equation in fluid mechanics It was derived from thermodynamics' first law. According to this law, the thermodynamic system's surroundings enhance internal energy while the amount of heat energy introduced to the system is less than the work the system performs.

$$\rho c_p\left(\frac{dT}{dt}\right) = \kappa\nabla^2 T + \tau.L.$$

$\boldsymbol{c_p}$ is specific heat, the thermal conductivity is denoted by $\boldsymbol{\kappa}$, $\boldsymbol{\tau}.\boldsymbol{L}$ signifies viscous dissipation.

2.19 Perturbation Method

A mathematical technique called the perturbation method is used to estimate solutions to difficult problems, especially in the domains of engineering, physics, and applied mathematics. It is particularly helpful for handling differential equation-based situations that are hard or impossible to answer precisely. In applied mathematics and engineering, the perturbation method

is a vital instrument that offers a systematic method for solving challenging issues. This approach makes it possible to obtain approximate solutions that are useful for comprehending how physical systems behave under little perturbations by adding a small parameter and growing the solution in a series.

2.20 Heat Flux

The rate of heat energy transmission per unit area in a specific direction is termed as the heat flux. Heat flux is a vector quantity used in fluid dynamics and thermodynamics to describe the movement of thermal energy caused by a temperature difference**.**

2.21 Velocity Field

The velocity of fluid particles at different places in space and time is represented mathematically by a velocity field. It shows how a flow field's velocity vector, which includes both speed and direction varies. It gives a thorough explanation of the flow pattern of a fluid at each location.

2.22 Lubrication Approach Theory

In fluid dynamics, this theory explains the fluids flow in thin layers. This approach is particularly useful in studying fluid flow between closely spaced surfaces.

CHAPTER NO 3

THE PERISTALTIC FLOW OF CHEMICALLY REACTIVE ELLIS FLUID THROUGH AN ASYMMETRIC CHANNEL HEAT AND MASS TRANSFER ANALYSIS

3.1 Introduction

A comprehensive discussion of the research work by Abbasi *et al.* [55] is given in this chapter. This study explored how the simultaneous transfer of heat and mass influenced Ellis fluid's peristaltic transport while considering no slip conditions. The study explores the peristaltic pattern of Ellis fluid in a channel, finding that fluid velocity decreases with higher fluid parameters and pressure rise improves with material parameters. The series solution of the generated differential system is derived using a regular perturbation strategy, and the temperature, heat transfer coefficient, axial velocity, and concentration are obtained.

3.2 Mathematical Formulation and Governing Equation

This study demonstrated heat and mass transmission of the peristaltic flow of chemically reactive Ellis fluid through asymmetric channel. The problem is described by following the governing equation

$$\boldsymbol{\nabla}.\boldsymbol{V}^* = 0, \tag{3.1}$$

$$\rho \frac{d\boldsymbol{V}^*}{dt^*} = -\nabla P^* + div\boldsymbol{S}^*, \tag{3.2}$$

$$\rho C_p \frac{dT^*}{dt^*} = k\nabla^{*2}T^* + T^*.\boldsymbol{\nabla}\boldsymbol{V}^*, \tag{3.3}$$

$$\frac{dC^*}{dt^*} = D\nabla^2 C^* - k_1(C^* - C_O^*), \tag{3.4}$$

where ρ is density velocity, the material derivative is $\frac{d}{dt^*}$, the temperature is T^*, the concentration is C^* the additional stress tensor $\boldsymbol{S}^*$, the hydrostatic pressure is P^*, and the thermal conductivity is k, concentration C^*, C_p is specific heat capacity , mass diffusivity chemical reaction is k_1.

Also, the Ellis model's stress tensor $\boldsymbol{S}^*$ is given as

$$\boldsymbol{S}^* = \frac{\mu}{1+\left(\frac{S}{\tau_0}\right)^{\alpha-1}} A_1 , \tag{3.5}$$

where

$$A_1 = (grad\, \boldsymbol{V}^*) + (grad\, \boldsymbol{V}^*)^T. \tag{3.6}$$

In the above tensor, the material constants are represented by (τ_o, α) and first Rivillin-Ericksen tensor by A_1.

Both channel boundaries are mathematically described as

$$H_1^* = d_1^* + a_1^* \cos\left[\frac{2\pi}{\lambda}(X^* - c^* t^*)\right], \tag{3.7}$$

$$H_2^* = -d_2^* - b_1^* cos\left[\frac{2\pi}{\lambda}(X^* - c^* t^*) + \phi\right]. \tag{3.8}$$

The phase difference with the wave amplitude (a_1^* , b_1^*) equals $(\emptyset)$, channel width is $(d_1^* + d_2^*)$ and wavelength is signified by λ. c is the speed of the sinusoidal wave train across the channel walls.

The suitable boundary conditions are

$$\left.\begin{array}{rr} U^* = 0, & at \quad H_1 , H_2, \\ T^* = T_1^*, \quad C^* = C_1^*, & at \quad H_1, \\ T^* = T_O^*, \quad C^* = C_O^*, & at \quad H_2. \end{array}\right\} \tag{3.9}$$

The *x* any y-components of the momentum equation are

$$\rho\left[\frac{\partial}{\partial t^*}+U^*\frac{\partial}{\partial X^*}+V^*\frac{\partial}{\partial Y^*}\right]U^*=-\frac{\partial P^*}{\partial X^*}+\frac{\partial S^*_{X^*X^*}}{\partial X^*}+\frac{\partial S^*_{X^*Y^*}}{\partial Y^*},\tag{3.10}$$

$$\rho\left[\frac{\partial}{\partial t^*}+U^*\frac{\partial}{\partial X^*}+V^*\frac{\partial}{\partial Y^*}\right]V^*=-\frac{\partial P^*}{\partial Y^*}+\frac{\partial S^*_{X^*Y^*}}{\partial X^*}+\frac{\partial S^*_{Y^*Y^*}}{\partial Y^*}.\tag{3.11}$$

The energy and concentration equations are

$$\rho C_P\left[\frac{\partial}{\partial t^*}+U^*\frac{\partial}{\partial X^*}+V^*\frac{\partial}{\partial Y^*}\right]T^*=D\left[\frac{\partial^2 T^*}{\partial X^{*2}}+\frac{\partial^2 T^*}{\partial Y^{*2}}\right]+S^*_{X^*Y^*}\frac{\partial U^*}{\partial X^*}+S^*_{Y^*Y^*}\frac{\partial V^*}{\partial Y^*}+\left(\frac{\partial V^*}{\partial X^*}+\frac{\partial U^*}{\partial Y^*}\right)S^*_{XY}\tag{3.12}$$

$$\left(\frac{\partial}{\partial t^*}+U^*\frac{\partial}{\partial X^*}+V^*\frac{\partial}{\partial Y^*}\right)C^*=D\left[\frac{\partial^2 C^*}{\partial X^{*2}}+\frac{\partial^2 C^*}{\partial Y^{*2}}\right]+\frac{DKT^*}{T^*_m}\left(\frac{\partial^2 T^*}{\partial X^{*2}}+\frac{\partial^2 T^*}{\partial Y^{*2}}\right)-k_1(C^*-C^*_O).\tag{3.13}$$

Taking into account the following transformation and non-dimensional parameters

$$x^*=X^*-c^*t^*,\quad y^*=Y^*,\qquad u^*=U^*-c^*,\qquad v^*=V^*,\qquad p^*(x)=P^*(X^*,t^*)$$

$$y^*=\frac{y^*}{d_1^*},\quad u^*=\frac{u^*}{C^*},\quad x^*=\frac{x^*}{\lambda},\ v^*=\frac{v^*}{C^*\delta},\quad \delta=\frac{d_1^*}{\lambda},\quad b=\frac{a_2^*}{d_1^*},\quad S^*=\frac{\mu\, c^*}{a},$$

$$\theta=\frac{T^*-T_0^*}{T^*-T_0^*},\quad P^*=\frac{d_1^2 p^*}{\lambda\mu c^*},\quad \psi^*=\frac{\psi^*}{c^* d_1^*},\qquad \emptyset=\frac{C^*-C_O^*}{C^*-C_O^*},\quad \mathrm{Re}=\frac{\rho c^* a_1}{\mu},\quad Sr=\frac{\rho DK(T_1^*-T_O^*)}{T_m^*\,\mu(C^*-C_O^*)},$$

$$Pr=\frac{\mu c^* P^*}{k},\ Sc=\frac{\mu}{P^* D},\quad \gamma=\frac{K_1 d^{*2}_1}{v},\ \mathrm{d}=\frac{d_2^*}{d_1^*},\quad h_1=\frac{H_1^*}{d_1^*},\quad h_2=\frac{H_2^*}{d_1^*},\tag{3.14}$$

where Sc is the Schmidt number, Prandtl number (Pr), wave number (δ), and *Re* is a Reynolds number. The dimensionless parameter of chemical reaction is represented by γ. The kinematic viscosity is represented by ν .

The use of non-dimensional quantities transforms the governing equation as

$$\delta\frac{\partial u^*}{\partial x^*}+\frac{\partial v^*}{\partial y^*}=0\,,\tag{3.15}$$

$$Re\left[\left(\delta u^{*}\frac{\partial}{\partial x^{*}}+v^{*}\frac{\partial}{\partial y^{*}}\right)u^{*}\right]=-\frac{\partial p^{*}}{\partial x^{*}}+\delta\frac{\partial}{\partial x^{*}}S_{x^{*}x^{*}}+\frac{\partial}{\partial y^{*}}S_{x^{*}y^{*}},\tag{3.16}$$

$$\delta\mathrm{Re}\left[\left(\delta u^{*}\frac{\partial}{\partial x^{*}}+v^{*}\frac{\partial}{\partial y^{*}}\right)v^{*}\right]=-\frac{\partial p^{*}}{\partial y}+\delta^{2}\frac{\partial S^{*}_{x^{*}y^{*}}}{\partial x^{*}}+\delta\frac{\partial S^{*}_{y^{*}y^{*}}}{\partial y^{*}},\tag{3.17}$$

$$S^{*}_{x^{*}x^{*}}=\frac{2\delta\frac{\partial u^{*}}{\partial x^{*}}}{1+(\beta X^{*})^{\alpha-1}},\tag{3.18}$$

$$S^{*}_{x^{*}y^{*}}=\frac{\left(\frac{\partial u^{*}}{\partial y^{*}}+\delta\frac{\partial v^{*}}{\partial x^{*}}\right)}{1+(\beta X^{*})^{\alpha-1}},\tag{3.19}$$

$$S^{*}_{y^{*}y^{*}}=\frac{2\frac{\partial v^{*}}{\partial y^{*}}}{1+(\beta X^{*})^{\alpha-1}},\tag{3.20}$$

where

$$X^{*}=\left[\frac{1}{2}(s^{*}_{x^{*}x^{*}})^{2}+2\left(s^{*}_{x^{*}y^{*}}\right)^{2}+\left(s^{*}_{y^{*}y^{*}}\right)^{2}\right]^{\frac{1}{2}}.$$

The temperature and concentration equations in non-dimensional form are

$$\mathrm{Re}\left[\left(\delta u^{*}\frac{\partial}{\partial x^{*}}+v^{*}\frac{\partial}{\partial y^{*}}\right)\theta\right]=\frac{1}{Pr}\left(\frac{\partial^{2}}{\partial x^{*2}}+\frac{\partial^{2}}{\partial y^{*2}}\right)\theta+Ec\left[\delta\frac{\partial u^{*}}{\partial x^{*}}\left(S^{*}_{x^{*}x^{*}}-S^{*}_{y^{*}y^{*}}\right)+\left(\delta\frac{\partial v^{*}}{\partial x^{*}}+\frac{\partial u^{*}}{\partial y^{*}}\right)S^{*}_{x^{*}y^{*}}\right],\tag{3.21}$$

$$\mathrm{Re}\left[\left(\delta u^{*}\frac{\partial}{\partial x^{*}}+v^{*}\frac{\partial}{\partial y^{*}}\right)\emptyset\right]=\frac{1}{Sc}\left(\delta^{2}\frac{\partial^{2}\emptyset}{\partial x^{*2}}+\frac{\partial^{2}\emptyset}{\partial y^{2}}\right)+Sr\left(\delta^{2}\frac{\partial^{2}\theta}{\partial x^{*2}}+\frac{\partial^{2}\theta}{\partial y^{2}}\right)-\gamma\emptyset\,.\tag{3.22}$$

Making use of the following stream functions in the above equations to reduce the dependent variables.

$$u^{*}=\frac{\partial\psi^{*}}{\partial y^{*}}\qquad\text{and}\quad v^{*}=-\delta\frac{\partial\psi^{*}}{\partial x^{*}}.\tag{3.23}$$

After dropping the asterisk, the ruling equations are given as

$$\mathrm{Re}\delta\left[\left(\frac{\partial}{\partial x}\frac{\partial\psi}{\partial y}-\frac{\partial}{\partial y}\frac{\partial\psi}{\partial x}\right)\frac{\partial\psi}{\partial y}\right]=-\frac{\partial p}{\partial x}+\delta\frac{\partial S_{xx}}{\partial x}+\frac{\partial S_{xy}}{\partial y},\tag{3.24}$$

$$\mathrm{Re}\delta^{2}\left[\left(\frac{\partial}{\partial x}\frac{\partial\psi}{\partial y}-\frac{\partial}{\partial y}\frac{\partial\psi}{\partial x}\right)\frac{\partial\psi}{\partial x}\right]=-\frac{\partial p}{\partial y}+\delta^{2}\frac{S_{xy}}{\partial x}+\delta\frac{\partial S_{yy}}{\partial y},\tag{3.25}$$

$$S_{xx} = \frac{2\delta\frac{\partial^2\psi}{\partial y}}{1+(\beta X)^{\alpha-1}}\,, \tag{3.26}$$

$$S_{xy} = \frac{\left(\frac{\partial^2\psi}{\partial y}-\delta^2\frac{\partial^2\psi}{\partial x^2}\right)}{1+(\beta X)^{\alpha-1}}\,, \tag{3.27}$$

$$S_{yy} = \frac{-2\delta\frac{\partial\psi}{\partial y\partial x}}{1+(\beta X)^{\alpha-1}}, \tag{3.28}$$

$$\mathrm{Re}\delta\left(\frac{\partial\psi}{\partial y}\frac{\partial}{\partial x}-\frac{\partial\psi}{\partial x}\frac{\partial}{\partial y}\right)\theta = \frac{1}{Pr}\left(\frac{\partial^2}{\partial x^2}+\frac{\partial^2}{\partial y^2}\right)\theta + Ec\left[\delta\frac{\partial u}{\partial x}\left(s_{xx}-s_{yy}\right)+\left(\delta\frac{\partial^2\psi}{\partial x^2}+\frac{\partial^2\psi}{\partial y^2}\right)S_{xy}\right], \tag{3.29}$$

$$\mathrm{Re}\delta\left(\frac{\partial\psi}{\partial y}\frac{\partial\emptyset}{\partial x}-\frac{\partial\psi}{\partial x}\frac{\partial\emptyset}{\partial y}\right) = \frac{1}{Sc}\left(\frac{\partial^2\emptyset}{\partial x^2}+\frac{\partial^2\emptyset}{\partial y^2}\right) = \frac{1}{Sc}\left(\frac{\partial^2\emptyset}{\partial x^2}+\frac{\partial^2\emptyset}{\partial y^2}\right)+ Sr\left(\delta^2\frac{\partial^2\emptyset}{\partial x^2}+\frac{\partial^2\emptyset}{\partial y^2}\right)-\gamma\emptyset\,. \tag{3.30}$$

3.3 Exact solution

Assuming the lubrication approach in the above modeled equations, (3.24) - (3.30) are simplified as follows:

$$\frac{\partial p}{\partial x} = \frac{\partial S_{xy}}{\partial y}, \tag{3.31}$$

$$\frac{\partial p}{\partial y} = 0, \tag{3.32}$$

$$S_{xy} = S_{yy} = 0\,, \tag{3.33}$$

$$S_{xy} = \frac{\left(\frac{\partial^2\psi}{\partial y^2}\right)}{1+(\beta X)^{\alpha-1}}, \tag{3.34}$$

$$\frac{\partial^2\theta}{\partial y^2} + Br\frac{\partial\psi^2}{\partial y^2}S_{xy} = 0, \tag{3.35}$$

$$\frac{\partial^2\emptyset}{\partial y^2} - Sc\,\gamma\emptyset + ScSr\frac{\partial^2\theta}{\partial y^2} = 0\,. \tag{3.36}$$

The non-dimensional boundary conditions are

$$\left.\begin{array}{c} \psi = \frac{F}{2}, \quad at \quad y = h_1 = 1 + cos2\pi x, \\ \psi = -\frac{F}{2}, \quad at \quad y = h_2 = -d - bcos[2\pi x + \varphi], \\ \frac{\partial \psi}{\partial y} = -1, \quad at \quad y = h_1, \quad y = h_2, \\ \theta = 0, \quad \emptyset = 0 \quad , y = h_2 \ , \ \theta = 1, \emptyset = 1 \quad , y = h_1. \end{array}\right\} \tag{3.37}$$

Pressure expression is considered constant so equation (3.31) integrates with respect *x*.

$$\frac{dp}{dx} y + C_2 = S_{xy}, \tag{3.38}$$

$$C_1 y + C_2 = S_{xy}, \tag{3.39}$$

where

$$\frac{dp}{dx} = C_1 \tag{3.40}$$

Putting in the equation and integrating it twice

$$\psi = \frac{y^3}{6} C_1 + \frac{\beta^{\alpha-1}(C_1 y + C_2)^{\alpha+2}}{C_1^2(\alpha + 1\,)(\alpha + 2\,)} + C_3 y + C_4, \tag{3.41}$$

where C_1, C_2, C_3, C_4 are constants, $\frac{dp}{dx}$ are nonlinear terms in constant.

The velocity profile of the fluid is given in the expression

$$u = \frac{\partial \psi}{\partial y} = \frac{y^2 C_1}{2} + \frac{\beta^{\alpha-1}(C_1 y + C_2)^{\alpha-1}}{C_1(\alpha + 1\,)} + C_3, \tag{3.42}$$

while flow rate is

$$Q = \int_{h_1}^{h_2} (U + 1\,) dy = \int_{h_2}^{h_1} U dy \ + \int_{h_2}^{h_1} dy \ , \tag{3.43}$$

$$Q = \frac{C_1}{8}(h_1^4 + h_2^4) + \frac{\beta^{\alpha-1}(C_1 h_1 + C_2)^{2\alpha-1}}{C_1^2(\alpha + 1\,)} - \frac{\beta^{\alpha-1}(C_1 h_2 + C_2)^{2\alpha-1}}{C_1^2(\alpha + 1)} - C_3(h_1 - h_2) + h_1 - h_2\,. \tag{3.44}$$

$$Q = q + 1 + d. \tag{3.45}$$

3.4 Results and Discussion

The physical explanation of the parameters behavior as it links to the velocity, concentration distribution ϕ, temperature distribution θ and pressure p, is the focus of this section. The velocity profile u for the conduct of different factors is plotted in figures 3.1 – 3.3. In figures 3.4 – 3.5, the effects of various parameters on the pressure rise Δp are examined. Figures 3.6 – 3.7, illustrate the impact of parameters on the temperature distribution while figures 3.8 – 3.10 demonstrate the concentration profile of the fluid with diverse parameters.

Figure 3.1. depicts the influence of the material parameter α on the velocity of the fluid. The velocity declines in the upper half of the channel while an opposite behavior can be seen in the lower half. The impact of Ellis parameter β is shown in Figure 3.2, when β is increased, axial velocity increases when moving higher to a lower region in fluid as shown in Figure 3.2. Additionally, it can be seen that velocity decreases close to the upper channel as the viscous behavior of the fluid changes. Figure 3.3 depicts that the velocity declines near the lower wall as the phase angle ϕ enhances.

The impact of α and β on pressure rise per wavelength is shown in figure 3.5 and 3.6. The figure consists of three distinct regions. The area where the flow rate $\mathrm{Q} > 0$ and pressure $(\Delta p) > O$ is known as the peristaltic pumping region. In this region, to overcome the resistance provided by the pressure gradient, the fluid flows forward along the peristalsis of walls. For free pumping region $\Delta p = 0, \mathrm{Q} > 0$, fluid flow only happens when walls move peristaltically and the last region, which is referred as the argument pumping region $\Delta p < 0$. It can be perceived from figure 3.5, as α increases, the pressure increases per wavelength in the peristaltic pumping area with a given value-defined flow rate. It can be witnessed in figure 3.5 that the impact of β, the second liquid constant that specifies the Ellis fluid model, is the opposite of that of α.

The distribution of temperature θ against y is shown in figures 3.6 and 3.7. These graphs show that raising α and β have varied effects on temperature. The fluid becomes more viscous as α increases. Due to the influence of β, temperature declines as depicted in figure 3.7.

Figure 3.8 deals with the concentration profile inspection. With the surge in the values of the Ellis parameter β, inclination in the concentration profile is observed. The chemical reaction parameter is signified by γ. Concentration profile grows (Figure. 3.9) as the chemical reaction parameter is enhanced due to surge in the rate of reaction. Figure 3.10 shows how the Schmidt number Sc influences the concentration to change. Since mass diffusivity is reduced, the profile shown exhibits a decreasing change in concentration with Schmidt number Sc.

3.5 Conclusion

Heat and mass transfer through the dynamics of an Ellis fluid through an asymmetric channel are investigated in the presence of a chemical reaction. The study concluded by emphasizing certain characteristics' importance in determining how Ellis fluid flow behaves. When the Ellis fluid parameter is raised, the bolus size close to the upper wall increases but fluid velocity decreases. A rising pressure with material quality indicates stronger resistance to fluid movement. While variations in the temperature field decrease the Prandtl number and the material constant, variations in the power-law index α enhance the temperature profile. Furthermore, the concentration falls as the Soret constant and Schmidt number rise, highlighting the interaction between mass diffusion and heat. Ultimately, as the phase angle increases, the bolus size decreases, highlighting the dynamic interplay of flow, thermal characteristics, and material factors. The optimization of fluid behavior in engineering and industrial applications can be greatly enhanced by these findings.

Graphs:

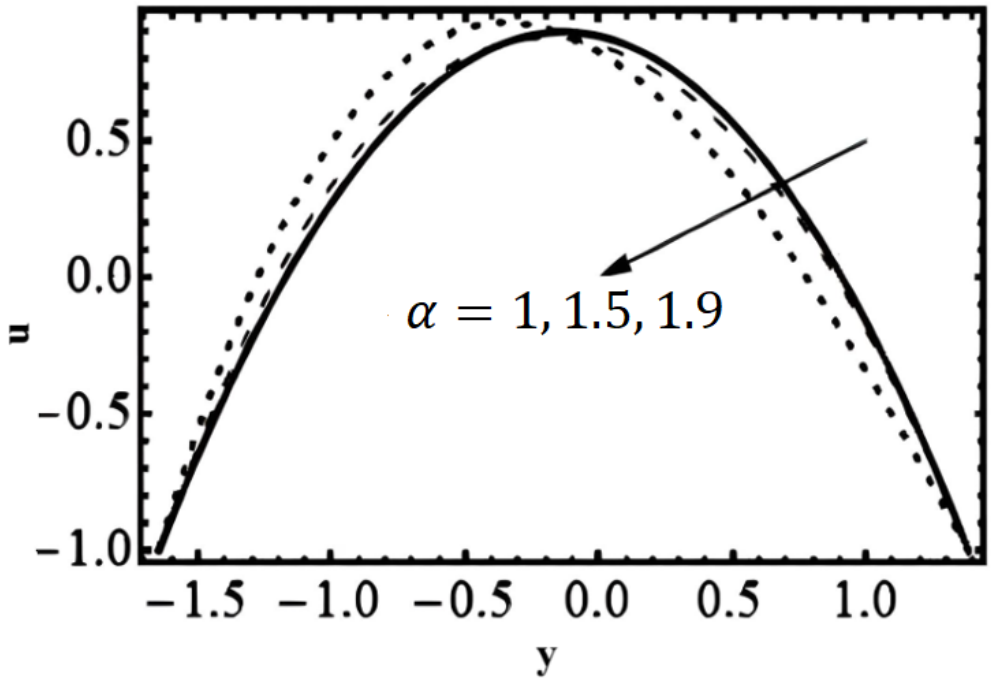

Fig. 3.1: Variation in the plots of velocity with diverse values of α.

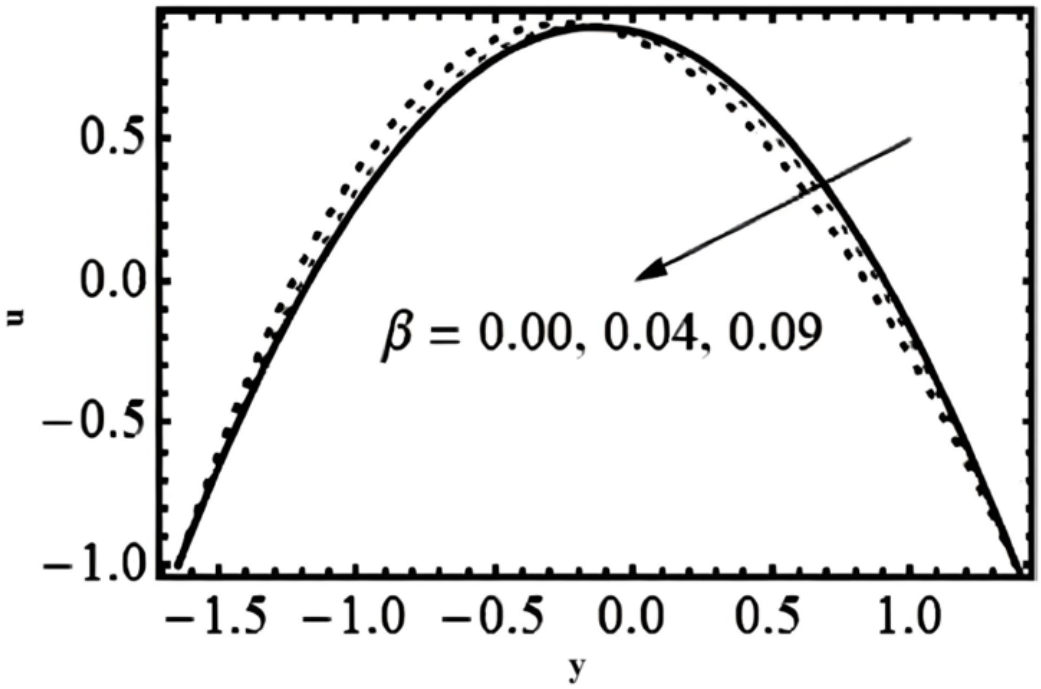

Fig. 3.2: Variation in the plots of velocity with diverse values of β.

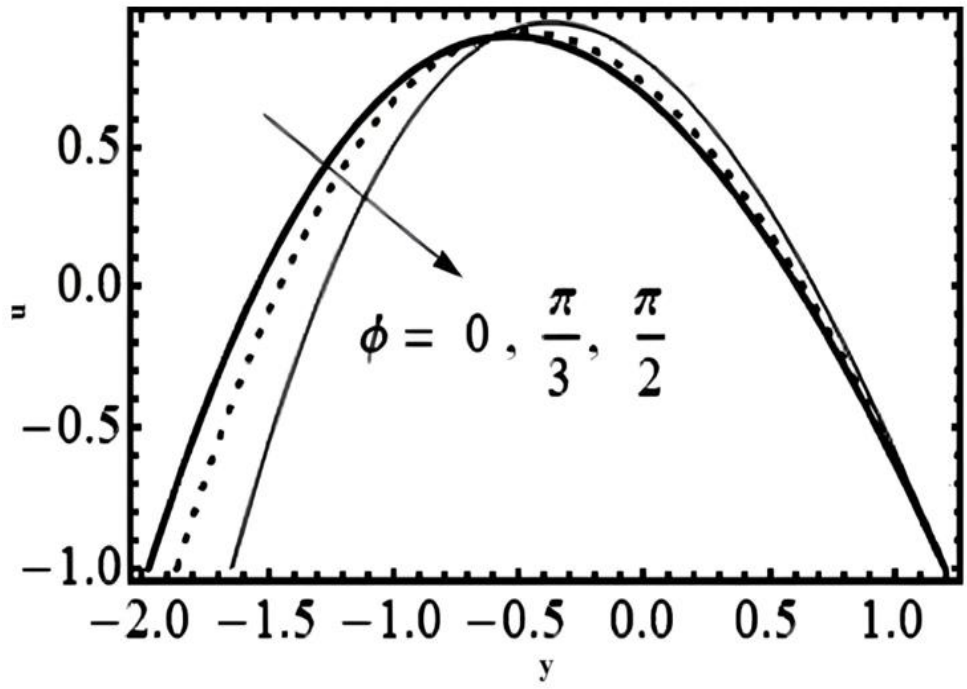

Fig. 3.3: Variation in the plots of velocity with diverse values of ϕ.

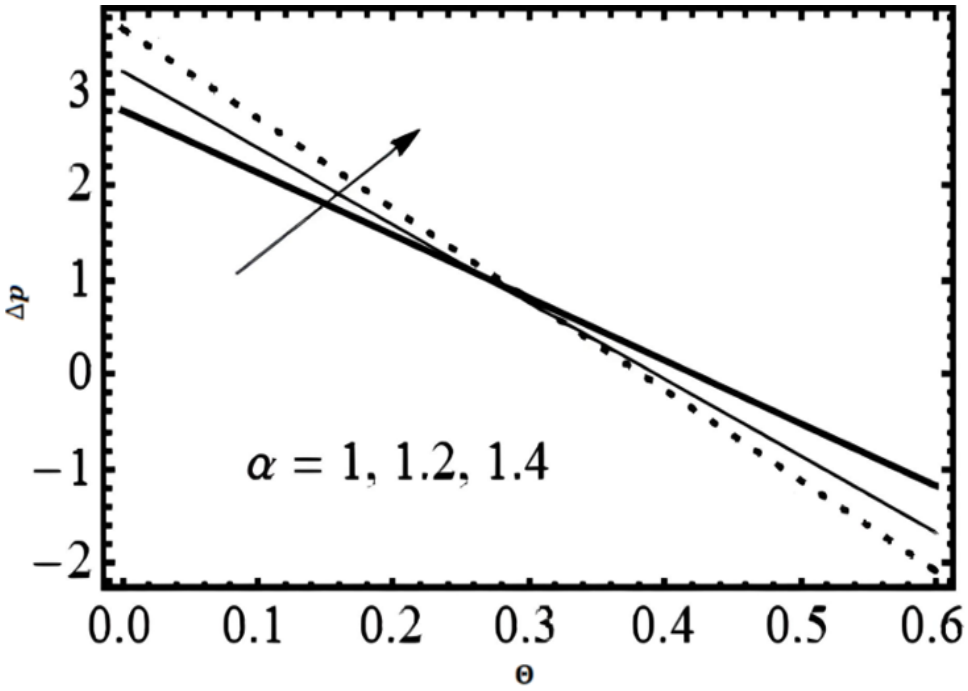

Fig 3.4: Variation in the plots of Δp with diverse values of α.

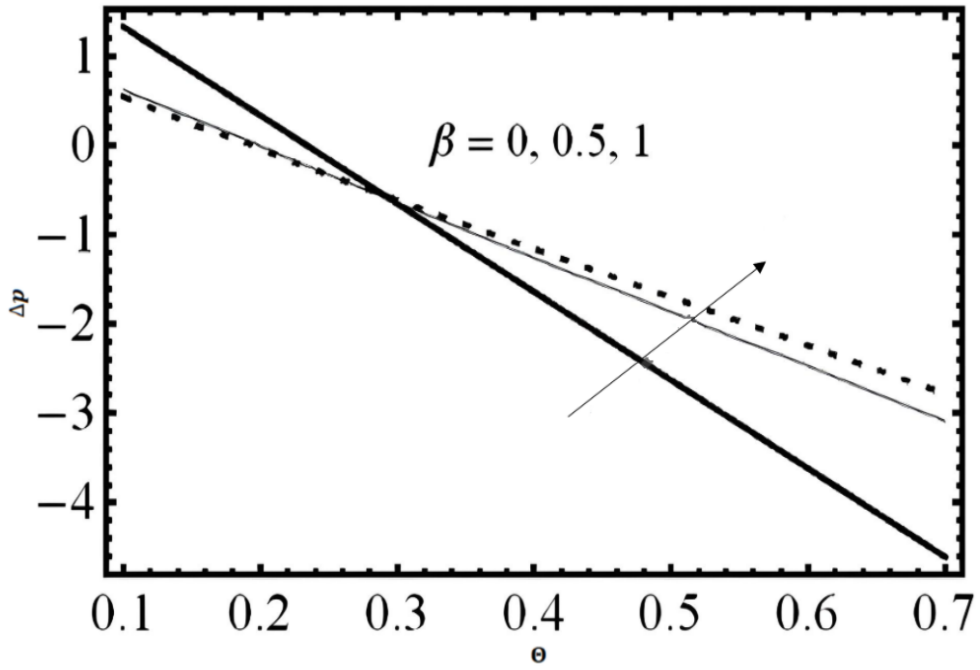

Fig. 3.5: Variation in the plots of Δp with diverse values of β.

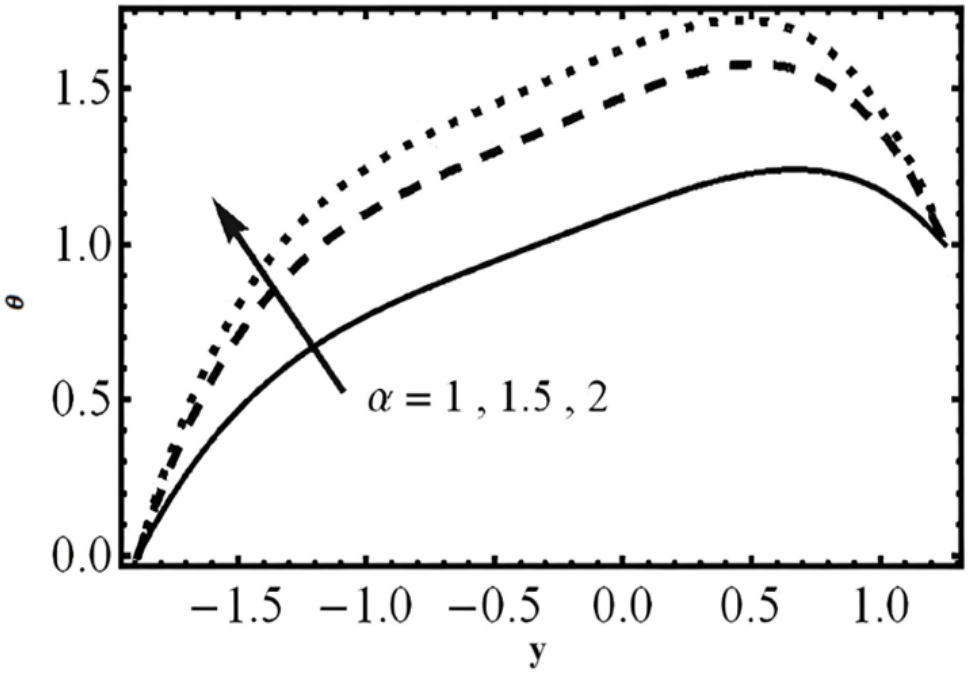

Fig.3.6: Variation in the plots of temperature with diverse values of α.

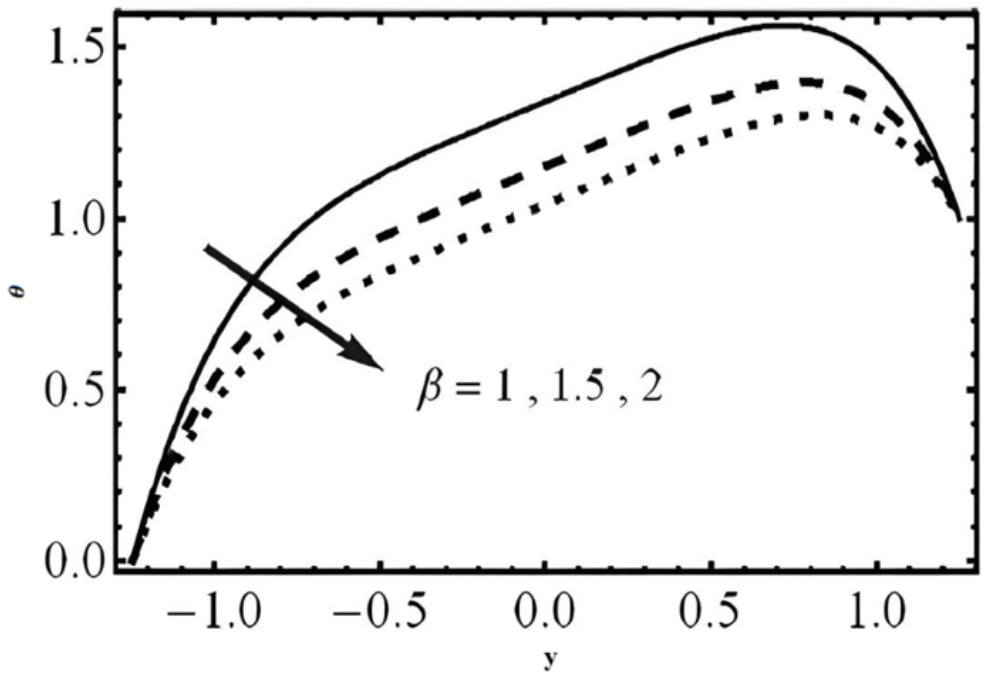

Fig.3.7: Variation in the plots of temperature with diverse values of β.

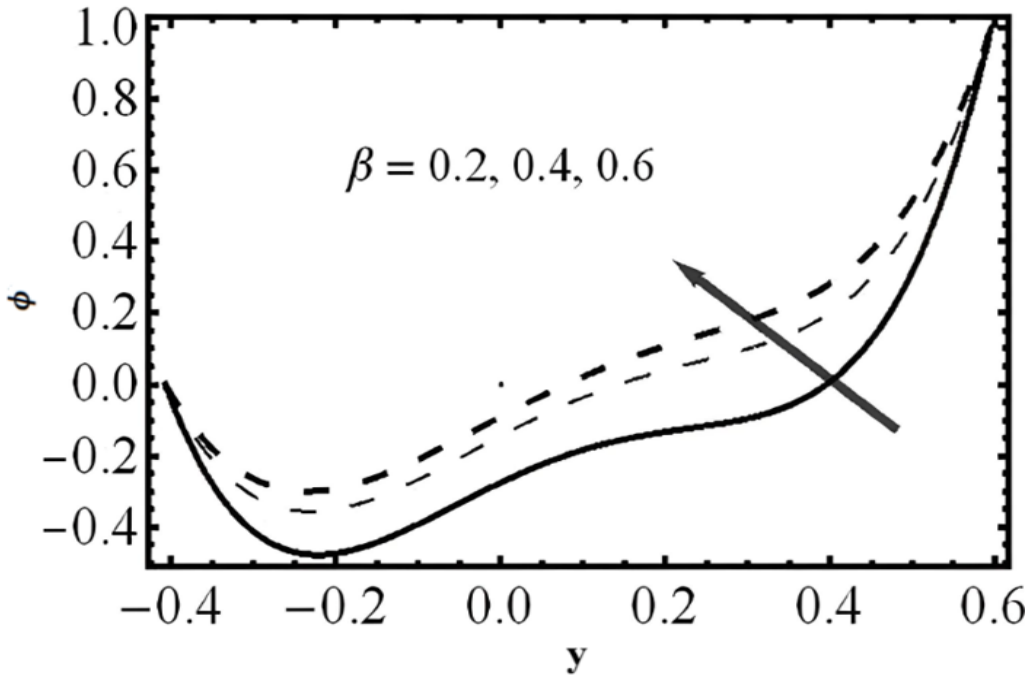

Fig.3.8: Variation in the plots of concentration with diverse values of β.

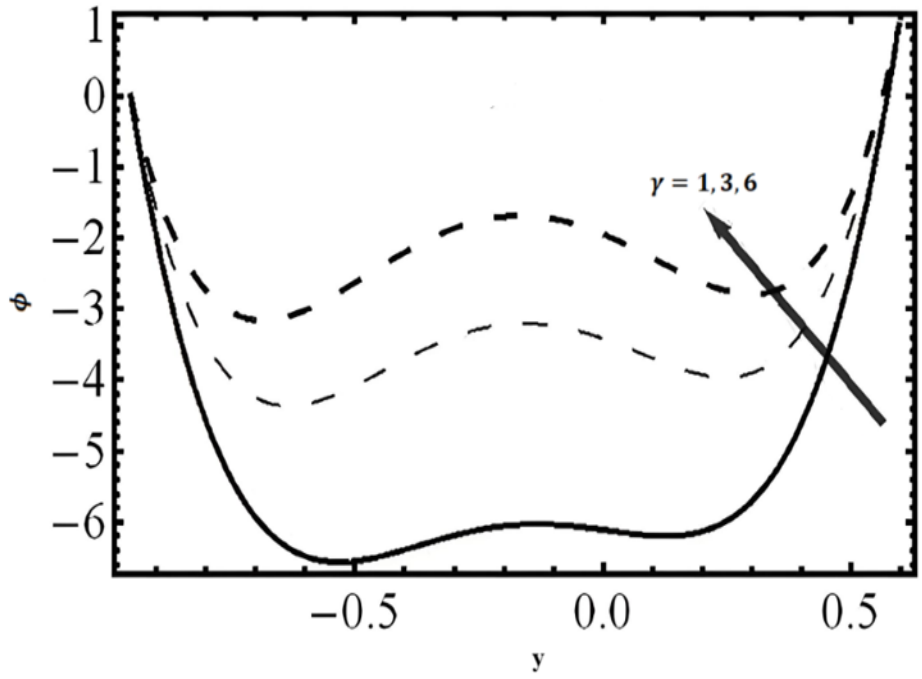

Fig.3.9: Variation in the plots of concentration with diverse values of γ.

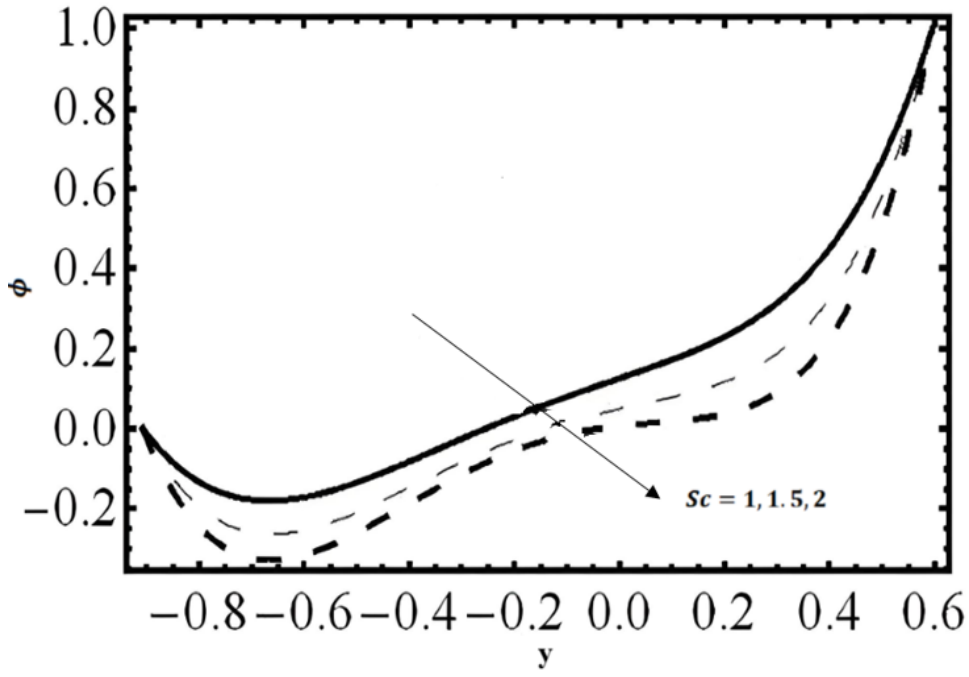

Fig.3.10: Variation in the plots of concentration with diverse values of Sc.

CHAPTER NO 4

ANALYSIS OF PERISTALTIC MHD ELLIS IN POROUS INCLINED ASYMMETRIC CHANNEL

4.1 Introduction

This study explores the characteristics of the laminar flow of Ellis fluid within a peristaltic flow in a porous, inclined, asymmetric tapered channel. The rheological equation is expressed in the Cartesian system, and the magnetohydrodynamics (MHD) and porosity effects are generated by the momentum equation's body force term. Profiles of temperature and velocity are used to display data visually. The problem's geometry is explained as follows:

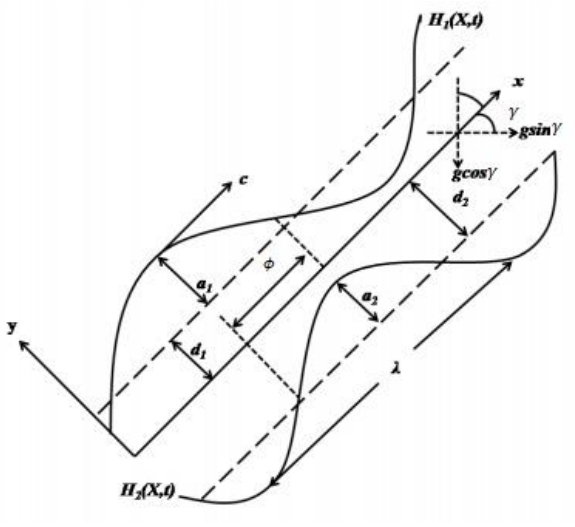

Fig. 4.1: Visual Framework of the Proposed Channel.

4.2 Problem Formation

This study investigates the peristaltic (MHD) Ellis fluid's mass and heat transport in a two-dimensional porous inclined asymmetry channel. Sinusoidal waves are produced through

maintaining a steady speed on the channel walls *c* by the fluid's electrical conductivity at a uniform magnetic and inclined angle. The geometry of walls is provided by

$$H_1(X,t) = d_1 + a_1 \sin\left[\frac{2\pi}{\lambda}(X - ct)\right], \tag{4.1}$$

$$H_2(X,t) = -d_2 - a_2 \sin\left[\frac{2\pi}{\lambda}(X - ct) + \phi\right], \tag{4.2}$$

where λ is the wavelength, t is a time, a_1, a_2 are the amplitudes, the channel's width is $d_1 + d_2$ and ϕ is a phase difference.

The velocity components are

$$\boldsymbol{V} = [U(x,y), V(x,y), 0]. \tag{4.3}$$

The ruling equations of the proposed model are given by

$$\boldsymbol{\nabla}.\boldsymbol{V} = 0, \tag{4.4}$$

$$\rho\frac{d\boldsymbol{V}}{dt} = div\,\boldsymbol{\tau} + \rho\boldsymbol{b}, \tag{4.5}$$

$$\rho c_p\frac{dT}{dt} = -div\,\boldsymbol{q} + \boldsymbol{\tau}.\boldsymbol{L}, \tag{4.6}$$

where

$$\boldsymbol{q} = -kgrad\,T.$$

The Ellis fluid model's equations that govern are provided by

$$\frac{\partial U}{\partial X} + \frac{\partial V}{\partial Y} = 0. \tag{4.7}$$

The equation for the x-component momentum is as follows:

$$\rho\left[\frac{\partial U}{\partial t} + U\frac{\partial U}{\partial X} + V\frac{\partial U}{\partial Y}\right] = -\frac{\partial P}{\partial X} + \frac{\partial S_{XX}}{\partial X} + \frac{\partial S_{XY}}{\partial Y} + \rho g sin\gamma - \sigma B_0^2 cos\theta[Ucos\theta - Vsin\theta] - \frac{\mu}{k_1}U. \tag{4.8}$$

The y-component momentum equation has been given as

$$\rho\left[\frac{\partial V}{\partial t}+U\frac{\partial V}{\partial X}+V\frac{\partial V}{\partial Y}\right]=-\frac{\partial P}{\partial Y}+\frac{\partial S_{XY}}{\partial X}+\frac{\partial S_{YY}}{\partial Y}-\rho g\cos\gamma+\sigma B_o^2 sin\theta(Ucos\theta-Vsin\theta)-\frac{\mu}{k_1}V\,. \tag{4.9}$$

The equation for energy is

$$\rho c_p\left[\frac{\partial T}{\partial t}+U\frac{\partial T}{\partial X}+V\frac{\partial T}{\partial Y}\right]=K\left(\frac{\partial^2 T}{\partial X^2}+\frac{\partial^2 T}{\partial Y^2}\right)+T_{XX}\frac{\partial U}{\partial X}+T_{YY}\frac{\partial V}{\partial Y}+T_{XY}\left(\frac{\partial V}{\partial X}+\frac{\partial U}{\partial Y}\right), \tag{4.10}$$

here c_p is specific heat capacity, K is the fluid's thermal conductivity, γ is the inclination of the channel, g is the acceleration due to the gravity, μ is viscosity, ρ is density, B_o is a magnetic field, θ is the inclination angle of the magnetic field.

The coordinates and velocities in two frames are defined by following the relations:

$$x=X-ct,\;\; y=Y,\;\;\; v=V,\; u=U-c.$$

The stream functions are given as

$$u=\frac{\partial\psi}{\partial y}\qquad\text{and}\qquad v=-\delta\frac{\partial\psi}{\partial x}. \tag{4.11}$$

For the dimensionless analysis process, we set up the following quantities

$$a=\frac{a_1}{d_1},\, b=\frac{a_2}{d_1},\, d=\frac{d_2}{d_1},\;\; y^*=\frac{y}{d_1},\;\; x^*=\frac{x}{\lambda},\, u^*=\frac{u}{c},\;\; v^*=\frac{v}{c},\;\; u=\frac{\partial\psi}{\partial y},\;\; v=-\frac{\partial\psi}{\partial x},$$

$$M^2=\frac{\sigma B_0^2 d_1}{\mu},\;\; Re=\frac{\rho c d_1}{\mu},\;\; h_1=\frac{H_1}{d_1},\;\; h_2=\frac{H_2}{d_1},\;\; \delta=\frac{d_1}{\lambda},\, t^*=\frac{ct}{\lambda},\;\; p^*=\frac{d_1^2 p}{c\lambda\mu},\;\; Fr=\frac{c^2}{g d_1},$$

$$k_1^*=\frac{k_1}{d_1^2},\;\; \mathrm{Br}=EcPr,\;\; \frac{T-T_0}{T_1-T_0}=\theta^*. \tag{4.12}$$

Re is the Reynold number, δ is the wave number, M is the Hartman number, and k_1 is the Darcy number. The Froude number is Fr, and the temperature distribution is denoted by θ^*. Pr is Prandtl number, and Ec is an Eckert number.

After utilizing the above quantities in the governing equations and by assuming the lubrication approach, we arrive at the following equations:

$$\frac{\partial p}{\partial x} = \frac{\partial T_{xy}}{\partial y} + \frac{sin\gamma}{Fr} - (M^2 \cos^2\theta)\frac{\partial \psi}{\partial y} - \frac{1}{k_1}\frac{\partial \psi}{\partial y}, \tag{4.13}$$

$$\frac{\partial p}{\partial y} = 0, \tag{4.14}$$

$$\frac{\partial^2 \theta}{\partial y^2} + Br\, T_{xy}\left(\frac{\partial^2 \psi}{\partial y^2}\right) = 0. \tag{4.15}$$

with

$$T_{xy} = \frac{\left(\frac{\partial^2 \psi}{\partial y^2}\right)}{1 + (\beta X)^{\alpha - 1}}.$$

The corresponding boundary conditions are:

$$\psi = \frac{F}{2}, \quad \frac{\partial \psi}{\partial y} = -1, \quad T = 0, \qquad at \qquad y = h_1(x), \tag{4.16}$$

$$\psi = -\frac{F}{2}, \quad \frac{\partial \psi}{\partial y} = -1, \quad T = 1, \qquad at \qquad y = h_2(x), \tag{4.17}$$

where

$$h_1(x) = 1 + \text{asin}(2\pi x),$$

$$h_2(x) = -d - bsin(2\pi x + \phi).$$

$$F = \int_{h_2(x)}^{h_1(x)} \frac{\partial \psi}{\partial y}\, dy. \tag{4.18}$$

Making use of the built-in tool NDSolve in MATHEMATICA software, the above modelled equations were numerically solved and graphs were plotted to check the results.

4.3 Results and Discussion

This section is dedicated to discuss the interpret the graphical results deduced by using the software to check the impact of diverse parameters on the velocity, pressure gradient and temperature profile of the proposed model. Fig. 4.2 – 4.5 are plotted to check the influence of parameters on the velocity of the fluid. Fig. 4.6 – 4.11 show the changes in the pressure gradient while with the impact of different attributes in it. Fig. 4.12 – 4.16 depict the temperature profile of the fluid.

Fig. 4.2 illustrates how the velocity profile decreases as the value of the parameter β increase. The viscous nature of the fluid changes with the increase in the β, thus causing fall in the velocity of the fluid. The increase in the porosity indicates more proportion of the void spaces in the channel, creating decline in the velocity as shown in the fig. 4.3. The other material parameter α shows a reverse result to β. Fluid flows with more velocity in the center of the channel with the increase in the values of α. The magnetic field creates a resistance in the flow of the fluid due to Lorentz force presence. The magnetic field parameter is denoted by M. Fig. 4.5 shows decline in the velocity with the growth in the values of M.

The amount of pressure change over a certain range is pressure gradient. It is crucial to study as it shows how quickly pressure enhances or declines in a certain direction. Fig. 4.6 shows surge in the pressure gradient by increasing the values of the material parameter α. Decline in the pressure gradient can be seen in fig. 4.7 due to increasing values of the magnetic parameter M. The Ellis fluid parameter β causes increase in the pressure gradient with growing values. The pressure gradient declines with the increasing values of the porosity parameter k_1 as demonstrated in the fig. 4.9. The ratio of inertial forces to gravitational forces is Froude number. Lower Froude number indicates that gravitational forces are dominating. Thus, increase in the pressure gradient can be observed in fig. 4.10. The inclination of the channel is signified by γ. Increase in the pressure gradient can be observed in fig. 4.11 by increasing the values of γ.

Fig. 4.12 shows the influence of the magnetic parameter on the temperature of the fluid. Temperature rises as the magnetic field parameter is growing. Growth in the temperature is

observed with the rising values of the Ellis fluid parameter. The shear thinning properties of the fluid enhances with the increased values of β thus, energy dissipation enhances and more heat conduction occurs in the fluid. Due to increased void spaces in the channel which slower down the fluid velocity. More heat energy is absorbed by the fluid causing rise in the temperature as shown in fig. 4.14. Influence of the material parameter α on the temperature profile can be seen in fig. 4.15. Decay in the temperature is observed with the growing values of α. Brinkman number helps us to understand the conversion of energy into heat in the fluid flow. Higher Brinkman number means that the viscous heating dominates thus resulting rise in the temperature as demonstrated in fig. 4.16.

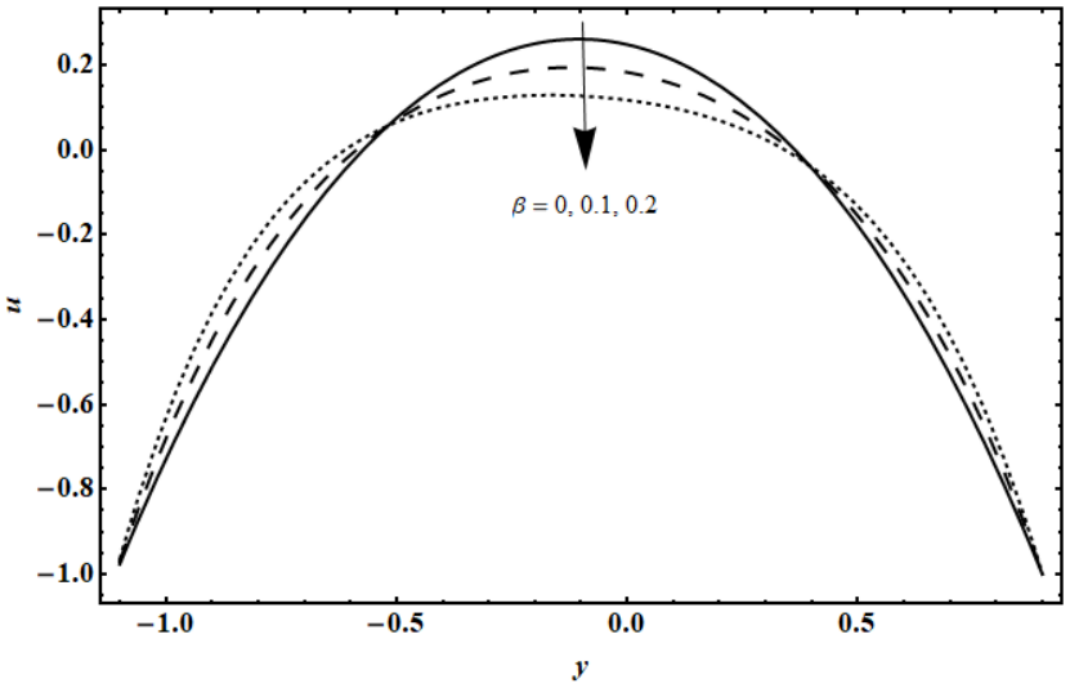

Fig. 4.2: Variation in the plots of velocity profile under the influence of β.

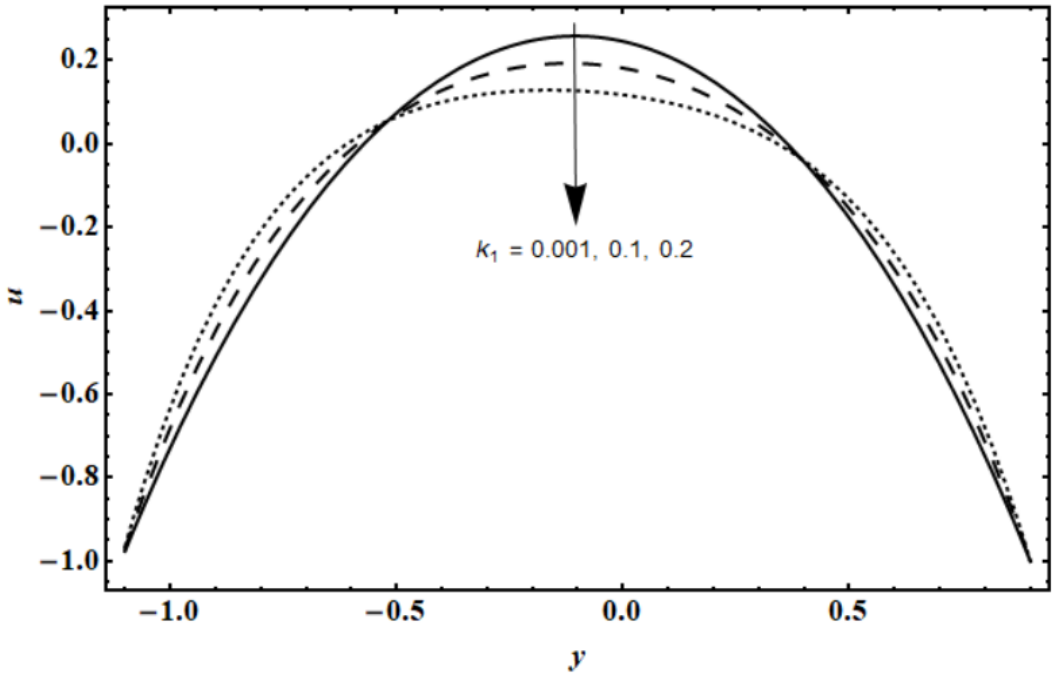

Fig. 4.3: Variation in the plots of velocity profile under the influence of k_1.

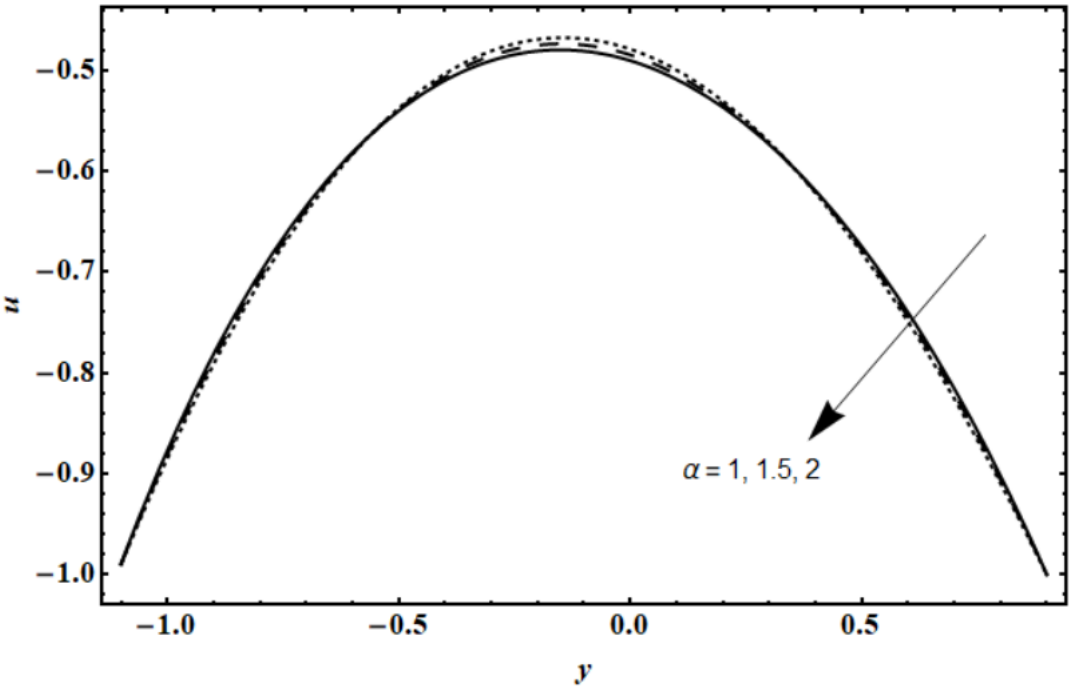

Fig. 4.4: Variation in the plots of velocity profile under the influence of α.

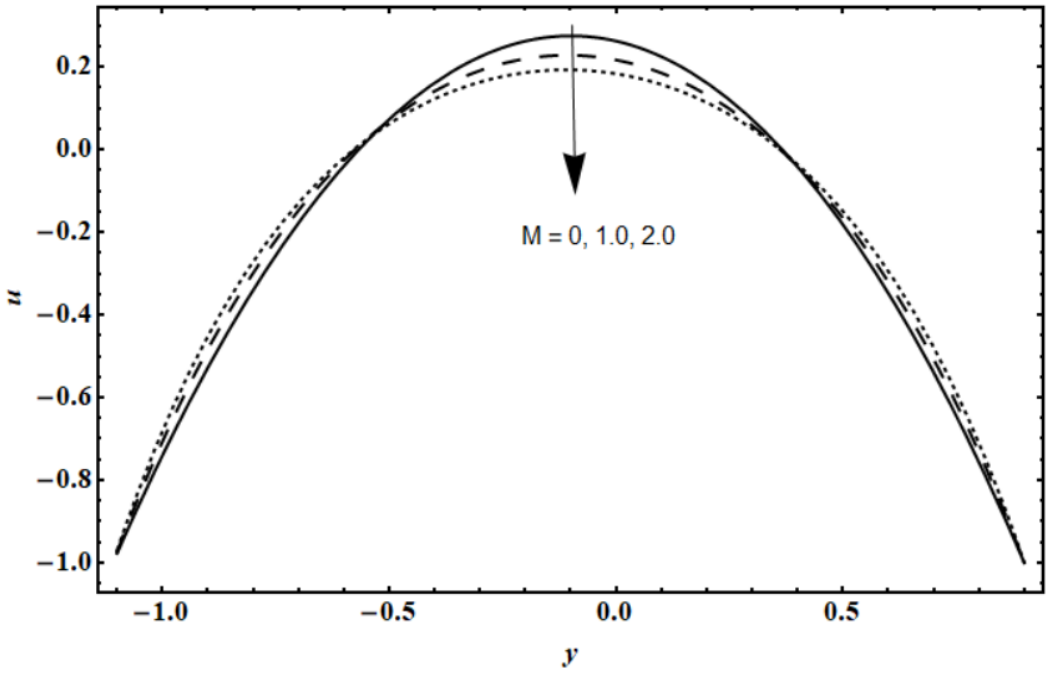

Fig. 4.5: Variation in the plots of velocity profile under the influence of M.

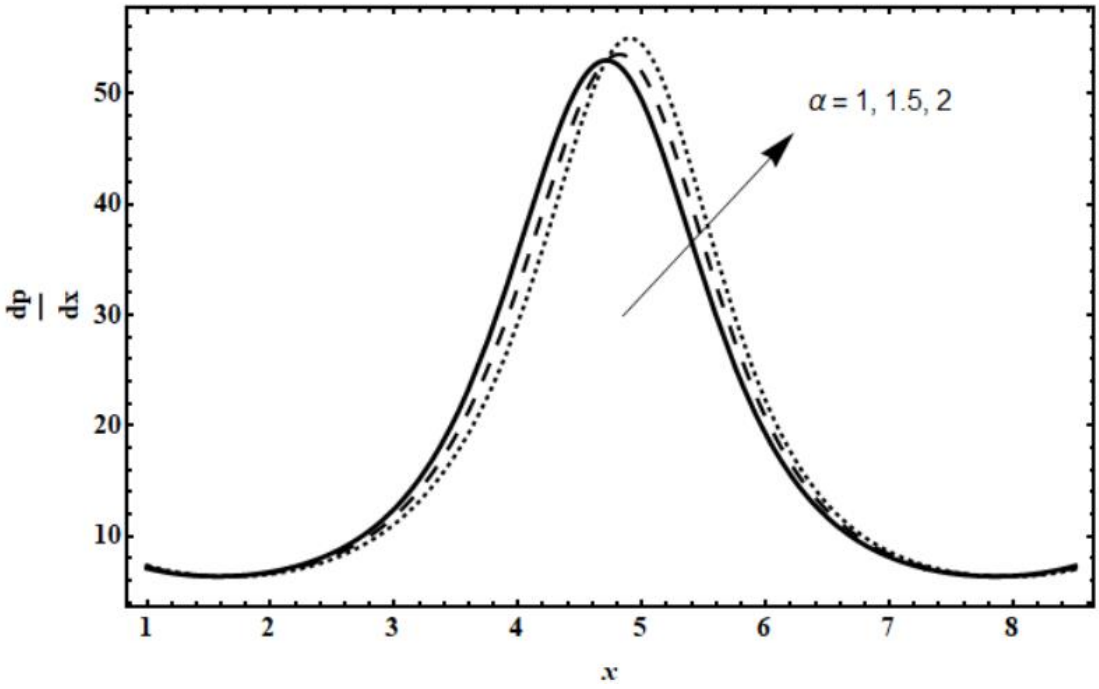

Fig. 4.6: Variation in the plots of pressure gradient under the influence of α.

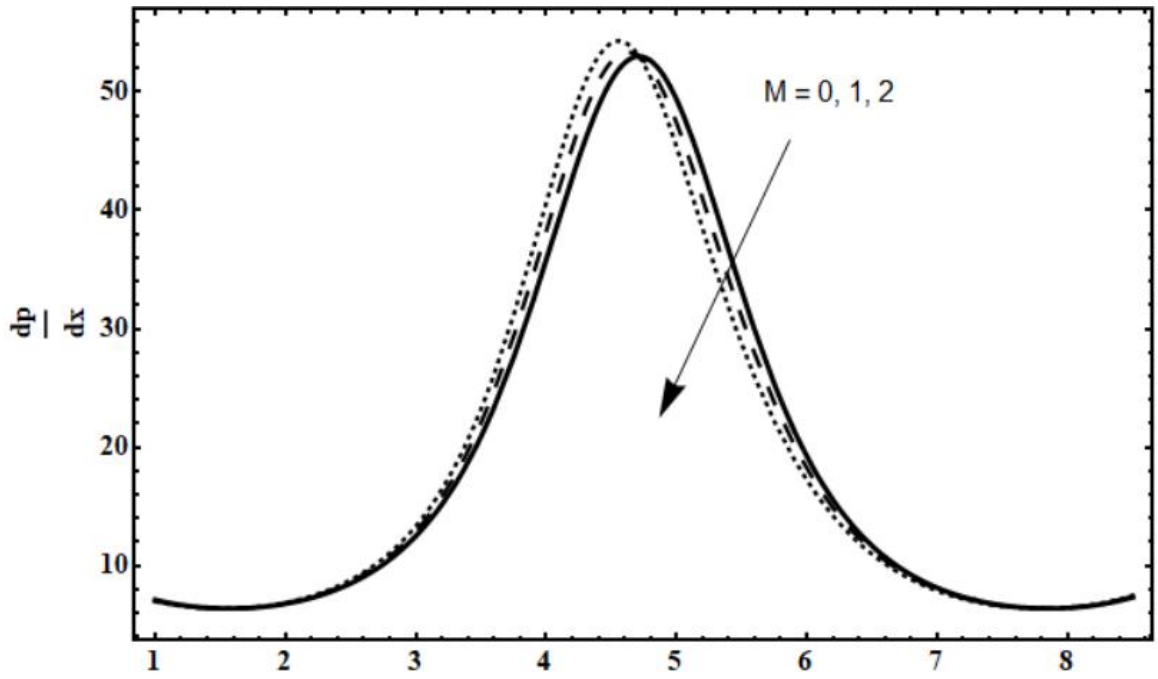

Fig. 4.7: Variation in the plots of pressure gradient under the influence of M.

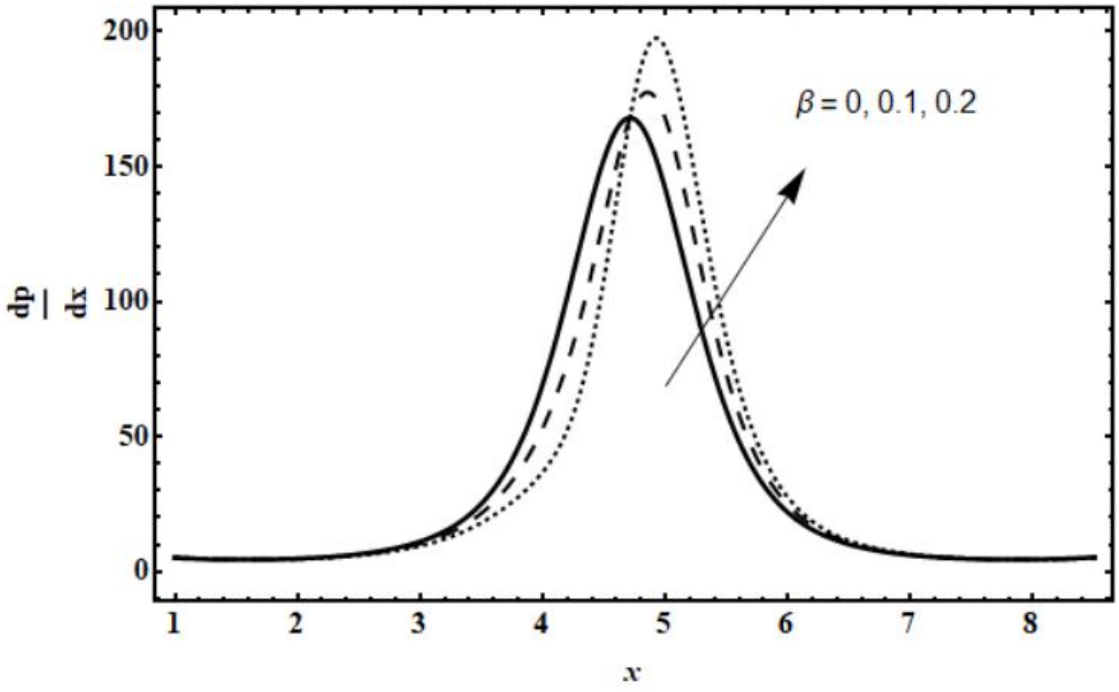

Fig. 4.8: Variation in the plots of pressure gradient under the influence of β.

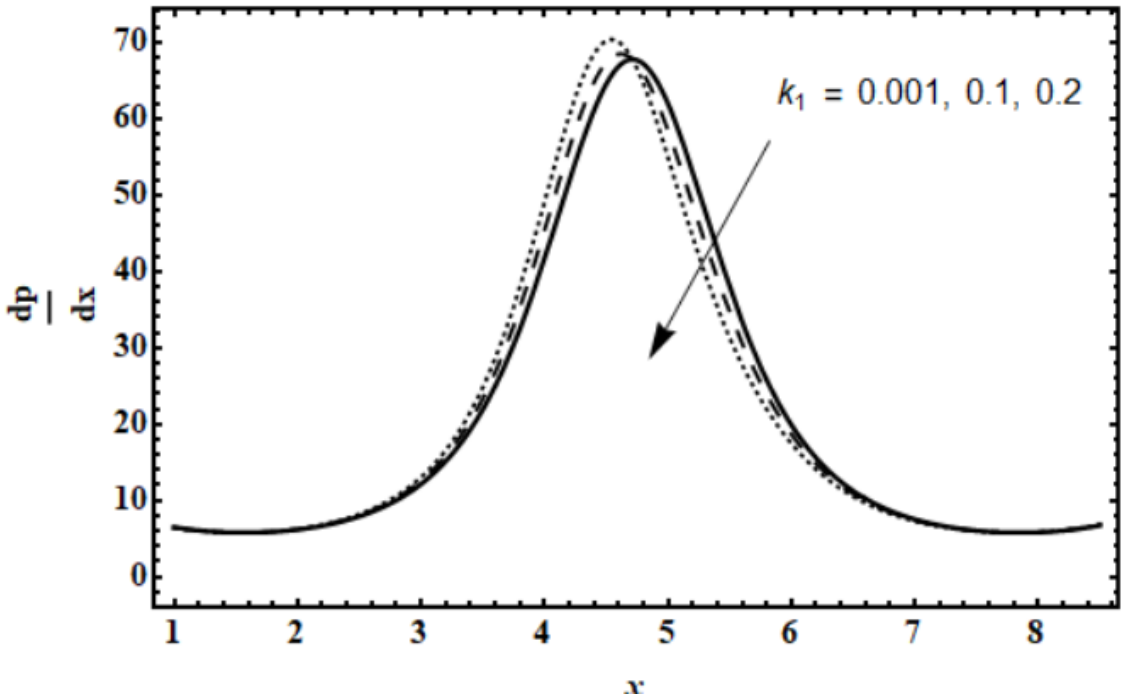

Fig. 4.9: Variation in the plots of pressure gradient under the influence of k_1.

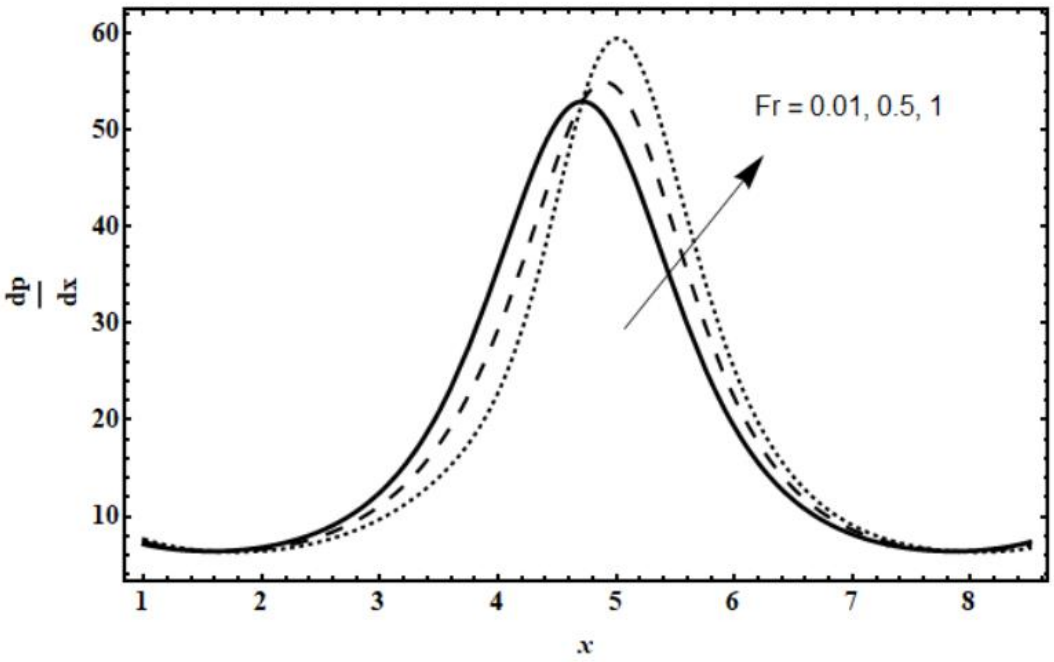

Fig. 4.10: Variation in the plots of pressure gradient under the influence of Fr.

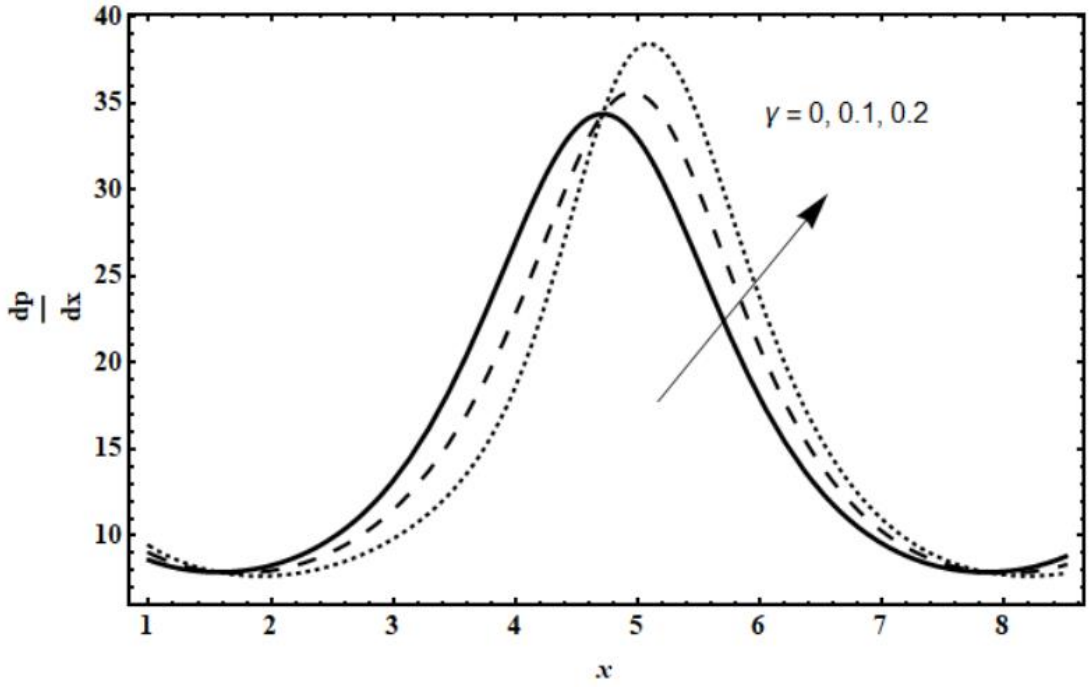

Fig. 4.11: Variation in the plots of pressure gradient under the influence of γ.

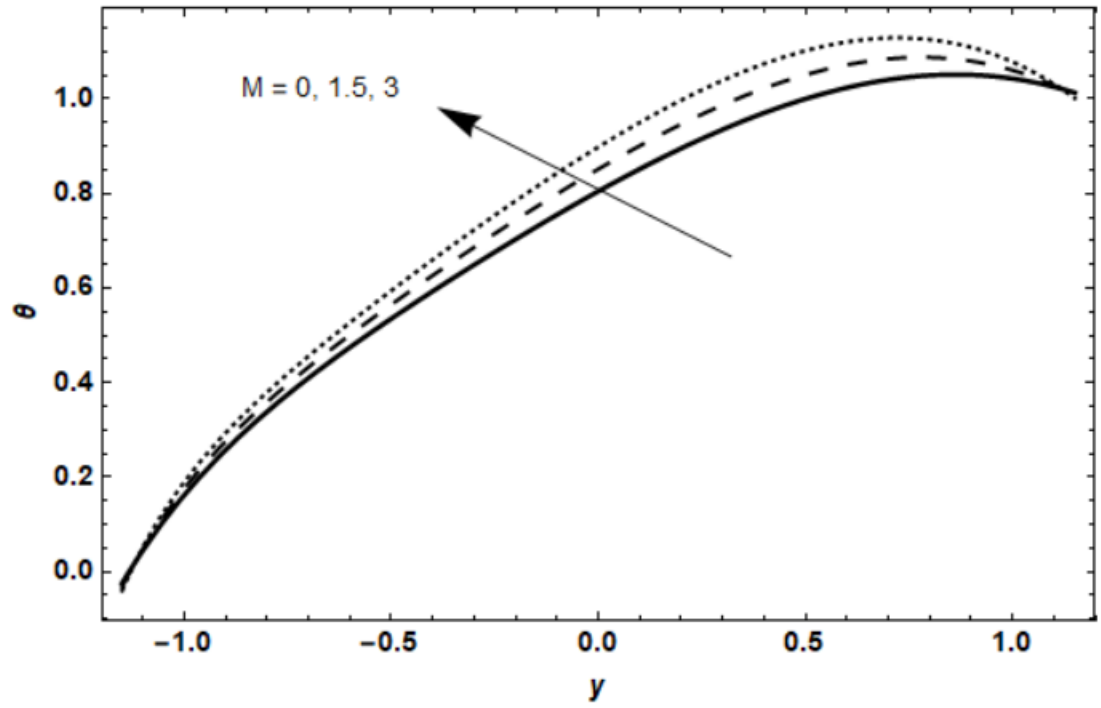

Fig. 4.12: Variation in the plots of temperature under the influence of M.

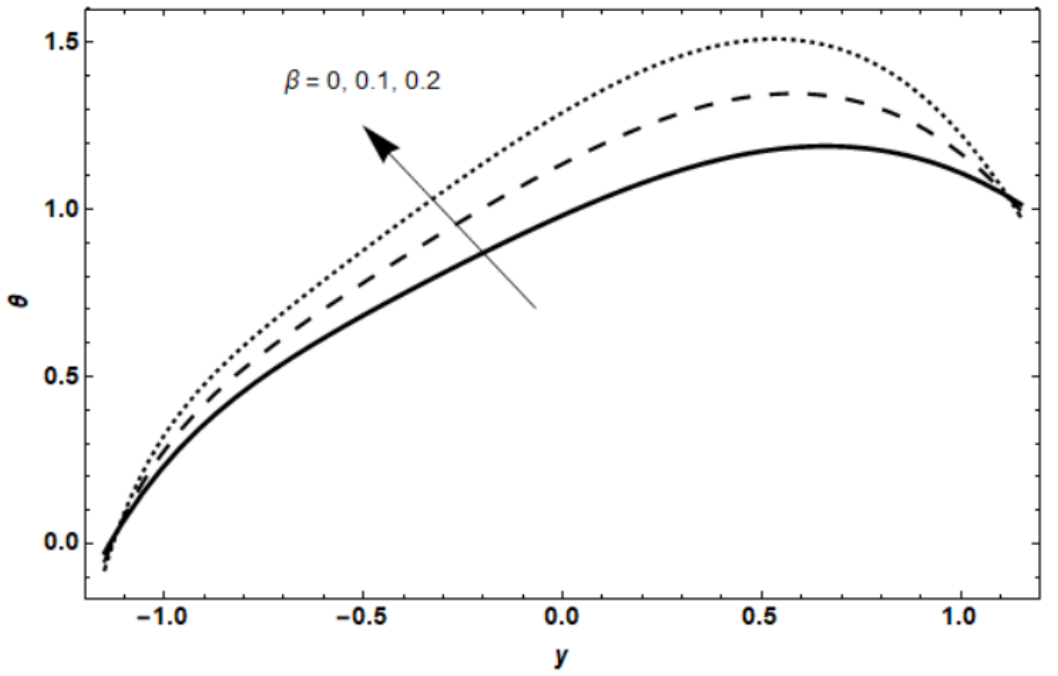

Fig. 4.13: Variation in the plots of temperature under the influence of β.

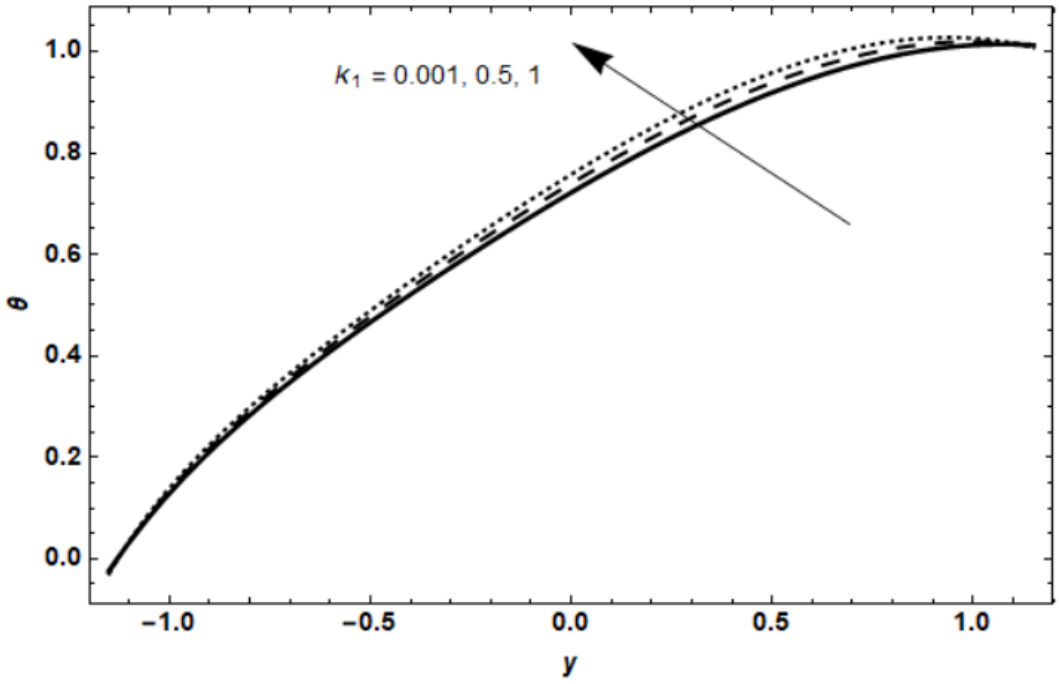

Fig. 4.14: Variation in the plots of temperature under the influence of k_1.

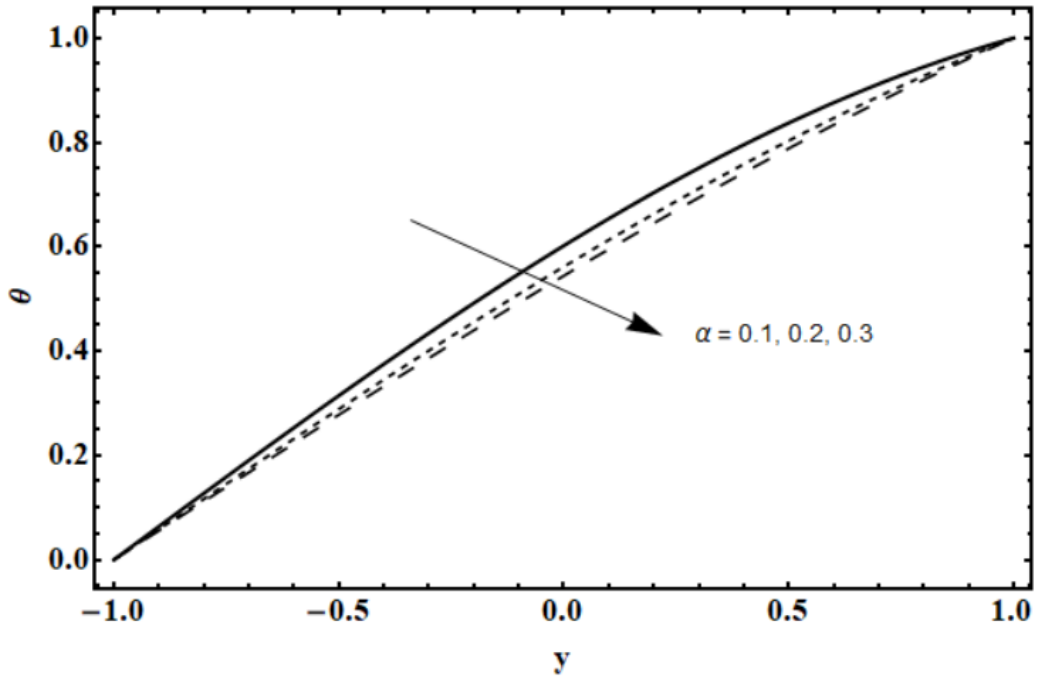

Fig. 4.15: Variation in the plots of temperature under the influence of α.

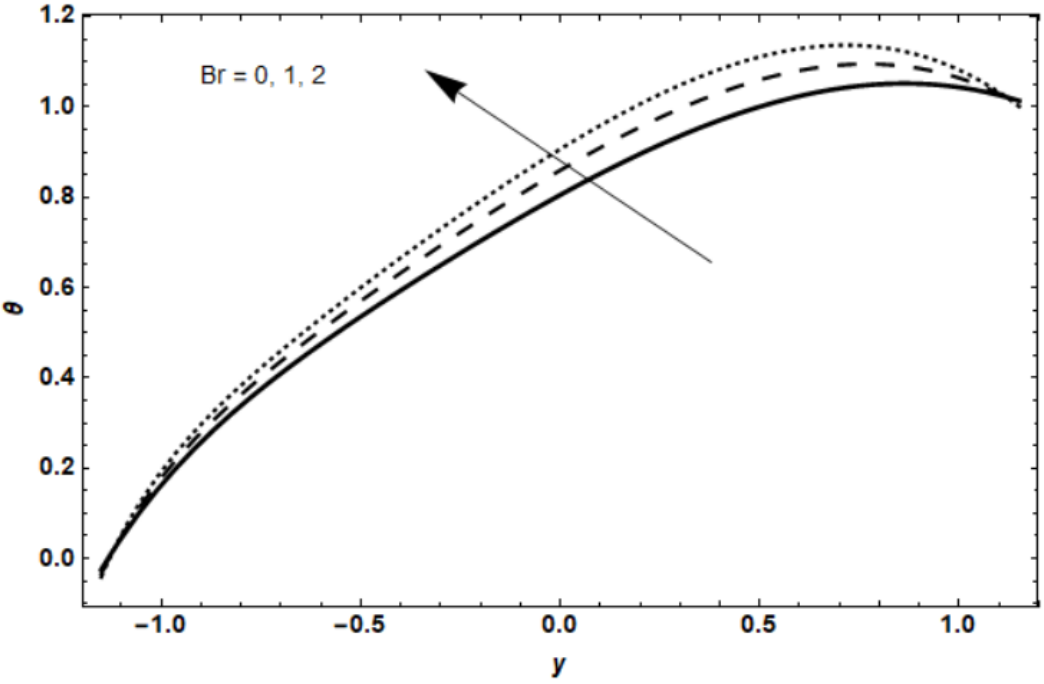

Fig. 4.16: Variation in the plots of temperature under the influence of Br.

CHAPTER NO 5

CONCLUSION AND FUTURE WORK

The peristaltic motion of an Ellis fluid in a porous, inclined asymmetric channel, while subjected to a magnetic field (MHD), is examined. The analysis takes into account how the fluid behaves when its rheology, channel inclination, magnetic field intensity, and porous medium permeability are all combined. Additionally, the Ellis fluid's non-Newtonian properties are crucial in determining the flow pattern, particularly in areas with low shear rates. The efficiency of pressure distribution flow is impacted by additional complications introduced by the channel's inclination angle and asymmetry. The results highlight how these parameters interact to maximize fluid flow in both industrial and biomedical settings.

The proposed model is formulated mathematically by using partial differential equations. Steam functions are utilized to reduce the number of dependent variables. Due to the complexity of the model, numerical approach has been used to obtain the graphical results.

Important findings show that the strength of the magnetic field has a major impact on fluid velocity, with higher magnetic intensity leading to flow retardation while the temperature enhanced and the pressure gradient declined. The increase in the porosity parameter resulted in decay of the velocity and pressure gradient while rise in the temperature occurred. Increase in the Ellis fluid parameter enhances the shear thinning properties of the fluid. Pressure gradient and temperature increased by increasing this parameter, while velocity declined. The material parameter has an opposite impact on the fluid’s velocity, pressure gradient and temperature than the Ellis fluid parameter β.

Future work

The study might be improved to include heat and mass transfer effects within the framework of peristaltic flow in order to better understand thermal and concentration gradients. Additionally,

magnetohydrodynamic (MHD) peristaltic flow systems can be simulated more accurately by including changeable magnetic field strength and direction. To determine whether elastic walls improve or hinder flow characteristics, it is crucial to look into how they affect fluid transport phenomena. Studying how nanoparticles, or nanofluids, affect fluid characteristics might also enhance system performance and heat transfer efficiency. To ensure practical application, experimental experiments are conducted to validate and corroborate theoretical and numerical conclusions. A more comprehensive knowledge of practical peristaltic flow applications in a variety of engineering and biomedical systems can be obtained by investigating three-dimensional flow geometries.

References

[1] T. W. Latham, “Fluid motions in a peristaltic pump,” Ph.D. dissertation, Massachusetts Institute of Technology, 1966.

[2] A. H. Shapiro, M. Y. Jaffrin, and S. L. Weinberg, “Peristaltic pumping with long wavelengths at low Reynolds number,” *J. Fluid Mech.*, vol. 37, no. 4, pp. 799–825, 1969.

[3] M. Y. Jaffrin and A. H. Shapiro, “Peristaltic pumping,” *Annu. Rev. Fluid Mech.*, vol. 3, no. 1, pp. 13–37, 1971.

[4] M. Mishra and A. R. Rao, “Peristaltic transport of a Newtonian fluid in an asymmetric channel,” *Z. Angew. Math. Phys.*, vol. 54, pp. 532–550, 2003.

[5] L. M. Srivastava and V. P. Srivastava, “Peristaltic transport of blood: Casson model—II,” *J. Biomech.*, vol. 17, no. 11, pp. 821–829, 1984.

[6] S. Nadeem and S. Akram, “Peristaltic flow of a Williamson fluid in an asymmetric channel,” *Commun. Nonlinear Sci. Numer. Simul.*, vol. 15, no. 7, pp. 1705–1716, 2010.

[7] A. M. El Misery, A. El Hakeem, A. El Naby, and H. El Nagar, “Effects of a fluid with variable viscosity and an endoscope on peristaltic motion,” *J. Phys. Soc. Jpn.*, vol. 72, no. 1, pp. 89–93, 2003.

[8] J. C. Burns and T. Parkes, “Peristaltic motion,” *J. Fluid Mech.*, vol. 29, no. 4, pp. 731–743, 1967.

[9] H. Vaidya, C. Rajashekhar, B. B. Divya, G. Manjunatha, K. V. Prasad, and I. L. Animasaun, “Influence of transport properties on the peristaltic MHD Jeffrey fluid flow through a porous asymmetric tapered channel,” *Results Phys.*, vol. 18, p. 103295, 2020.

[10] N. Ali and T. Hayat, “The peristaltic flow of a micropolar fluid in an asymmetric channel,” *Comput. Math. Appl.*, vol. 55, no. 4, pp. 589–608, 2008.

[11] S. Nadeem and S. Akram, “Peristaltic flow of a Williamson fluid in an asymmetric channel,” *Commun. Nonlinear Sci. Numer. Simul.*, vol. 15, no. 7, pp. 1705–1716, 2010.

[12] H. Alfvén, “Existence of electromagnetic-hydrodynamic waves,” *Nature*, vol. 150, no. 3805, pp. 405–406, 1942.

[13] M. Gnaneswara Reddy and K. Venugopal Reddy, “Influence of Joule heating on MHD peristaltic flow of a nanofluid with compliant walls,” *Procedia Eng.*, vol. 127, pp. 1002–1009, 2015.

[14] M. Rafiq, A. Shaheen, Y. Trabelsi, S. M. Eldin, M. Ijaz Khan, and D. K. Suker, “Impact of activation energy and variable properties on peristaltic flow through porous wall channel,” *Sci. Rep.*, vol. 13, no. 1, pp. 3219, 2023.

[15] M. Gnaneswara Reddy, “Velocity and thermal slip effects on MHD third order blood flow in an irregular channel through a porous medium with homogeneous/heterogeneous reactions,” *Nonlinear Eng.*, vol. 6, no. 3, pp. 167–177, 2017.

[16] F. M. Abbasi, T. Hayat, and B. Ahmad, “Peristaltic transport of copper–water nanofluid saturating porous medium,” *Physica E: Low-dimensional Syst. Nanostructures*, vol. 67, pp. 47–53, 2015.

[17] A. Ali, S. Saleem, S. Mumraiz, A. Saleem, M. Awais, and D. N. Khan Marwat, “Investigation on TiO2–Cu/H2O hybrid nanofluid with slip conditions in MHD peristaltic flow of Jeffrey material,” *J. Therm. Anal. Calorim.*, vol. 143, pp. 1985–1996, 2021.

[18] S. Srinivas and M. Kothandapani, “Peristaltic transport in an asymmetric channel with heat transfer—a note,” *Int. Commun. Heat Mass Transfer*, vol. 35, no. 4, pp. 514–522, 2008.

[19] S. E. Ahmed, A. A. Arafa, S. A. Hussein, and Z. A. Raizah, “Novel treatments for the bioconvective radiative Ellis nanofluids wedge flow with viscous dissipation and activation energy,” *Case Stud. Therm. Eng.*, vol. 40, pp. 102510, 2022.

[20] R. Saravana, S. Sreenadh, P. R. Kumar, and V. R. Babu, “Peristaltic pumping of Ellis fluid through a flexible tube with complete slip effects,” *J. Nav. Archit. Marine Eng.*, vol. 17, no. 2, 2020.

[21] J. Suresh Goud and R. Hemadri Reddy, “Peristaltic motion of an Ellis fluid model in a vertical uniform tube with wall properties,” *Int. J. Civ. Eng. Technol.*, vol. 9, pp. 847–856, 2018.

[22] Z. Asghar, R. A. Shah, W. Shatanawi, and N. Ali, “A theoretical approach to mathematical modeling of sperm swimming in viscoelastic Ellis fluid in a passive canal,” *Arch. Appl. Mech.*, vol. 93, no. 4, pp. 1525–1534, 2023.

[23] A. Small, P. Nagarani, and M. Narahari, “Peristaltic pumping of an Ellis fluid in an inclined asymmetric channel,” *J. Appl. Math. Informatics*, vol. 41, no. 1, pp. 51–70, 2023.

[24] M. A. Abbas, M. M. Bhatti, and M. M. Rashidi, “Peristaltic blood flow of Ellis fluid through a nonuniform channel having compliant walls,” *J. Nanofluids*, vol. 6, no. 2, pp. 318–323, 2017.

[25] M. N. Khan, N. Akkurt, N. A. Ahammad, S. Ahmad, A. Amari, S. M. Eldin, and A. A. Pasha, “Irreversibility analysis of Ellis hybrid nanofluid with surface catalyzed reaction and multiple slip effects on a horizontal porous stretching cylinder,” *Arabian J. Chem.*, vol. 15, no. 12, pp. 104326, 2022

[26] K. T. Kumar, A. Kavitha, and R. Saravana, “Peristaltic flow of an Ellis fluid model in an inclined uniform tube with wall properties,” *Int. J. Mech. Eng. Technol.*, vol. 9, pp. 15–27, 2018.

[27] E. F. El Shehawey and S. Z. A. Husseny, “Effects of porous boundaries on peristaltic transport through a porous medium,” *Acta Mech.*, vol. 143, no. 3, pp. 165–177, 2000.

[28] M. F. El-Sayed, N. T. M. Eldabe, A. Y. Ghaly, and H. M. Sayed, "Effects of chemical reaction, heat, and mass transfer on non-Newtonian fluid flow through porous medium in a vertical peristaltic tube," *Transport Porous Media*, vol. 89, pp. 185–212, 2011.

[29] K. S. Mekheimer, S. Z. A. Husseny, and Y. A. Elmaboud, "Effects of heat transfer and space porosity on peristaltic flow in a vertical asymmetric channel," *Numer. Methods Partial Differ. Equations*, vol. 26, no. 4, pp. 747–770, 2010.

[30] D. Tripathi and O. A. Bég, "A numerical study of oscillating peristaltic flow of generalized Maxwell viscoelastic fluids through a porous medium," *Transport Porous Media*, vol. 95, pp. 337–348, 2012.

[31] T. Hayat, M. Rafiq, and A. Alsaedi, "Investigation of Hall current and slip conditions on peristaltic transport of Cu-water nanofluid in a rotating medium," *Int. J. Therm. Sci.*, vol. 112, pp. 129–141, 2017.

[32] K. Vajravelu, G. Radhakrishnamacharya, and V. Radhakrishnamurty, "Peristaltic flow and heat transfer in a vertical porous annulus, with long wave approximation," *Int. J. Non-Linear Mech.*, vol. 42, no. 5, pp. 754–759, 2007.

[33] R. Bhargava, S. Sharma, H. S. Takhar, T. A. Beg, O. A. Bég, and T. K. Hung, "Peristaltic pumping of micropolar fluid in the porous channel—a model for stenosed arteries," *J. Biomech.*, vol. 39, p. S649, 2006.

[34] T. Hayat, M. U. Qureshi, and Q. Hussain, "Effect of heat transfer on the peristaltic flow of an electrically conducting fluid in a porous space," *Appl. Math. Model.*, vol. 33, no. 4, pp. 1862–1873, 200

[35] N. S. Akbar, S. Nadeem, T. Hayat, and A. A. Hendi, "Effects of heat and mass transfer on the peristaltic flow of hyperbolic tangent fluid in an annulus," *Int. J. Heat Mass Transfer*, vol. 54, no. 19–20, pp. 4360–4369, 2011.

[36] R. Ellahi, M. M. Bhatti, and K. Vafai, "Effects of heat and mass transfer on peristaltic flow in a non-uniform rectangular duct," *Int. J. Heat Mass Transfer*, vol. 71, pp. 706–719, 2014.

[37] A. Ogulu, “Effect of heat generation on low Reynolds number fluid and mass transport in a single lymphatic blood vessel with uniform magnetic field,” *Int. Commun. Heat Mass Transfer*, vol. 33, no. 6, pp. 790–799, 2006.

[38] S. Akram, M. Athar, K. Saeed, A. Razia, and T. Muhammad, “Hybridized consequence of thermal and concentration convection on peristaltic transport of magneto Powell–Eyring nanofluids in an inclined asymmetric channel,” *Math. Methods Appl. Sci.*, vol. 46, no. 10, pp. 11462–11478, 2023.

[39] M. Saleem, Q. M. Al-Mdallal, Q. A. Chaudhry, S. Noreen, and A. Haider, “Partial slip effects on the peristaltic motion of an upper-convected Maxwell fluid through an irregular channel,” *SN Appl. Sci.*, vol. 2, pp. 1–14, 2020.

[40] Z. Asghar and N. Ali, “Analysis of mixed convective heat and mass transfer on peristaltic flow of Fene-P fluid with chemical reaction,” *J. Mech.*, vol. 32, no. 1, pp. 83–92, 2016.

[41] N. T. Eldabe, M. A. Elogail, S. M. Elshaboury, and A. A. Hasan, “Hall effects on the peristaltic transport of Williamson fluid through a porous medium with heat and mass transfer,” *Appl. Math. Model.*, vol. 40, no. 1, pp. 315–328, 2016.

[42] S. A. Khan, T. Hayat, and A. Alsaedi, “Numerical study for entropy optimized radiative unsteady flow of Prandtl liquid,” *Fuel*, vol. 319, p. 123601, 2022.

[43] P. Tamizharasi, R. Vijayaragavan, and A. Magesh, “Heat and mass transfer analysis of the peristaltic driven flow of nanofluid in an asymmetric channel,” *Partial Differ. Equ. Appl. Math.*, vol. 4, p. 100087, 2021.

[44] H. S. Hina, S. M. Kayani, and M. Mustafa, “Aiding or opposing electro-osmotic flow of Carreau–Yasuda nanofluid induced by peristaltic waves using Buongiorno model,” *Waves Random Complex Media*, pp. 1–17, 2022.

[45] W. M. Hasona, A. A. El-Shekhipy, and M. G. Ibrahim, “Combined effects of magnetohydrodynamic and temperature-dependent viscosity on peristaltic flow of Jeffrey

nanofluid through a porous medium: Applications to oil refinement," *Int. J. Heat Mass Transfer*, vol. 126, pp. 700–714, 2018.

[46] K. Das, "Influence of slip and heat transfer on MHD peristaltic flow of a Jeffrey fluid in an inclined asymmetric porous channel," *Indian J. Math.*, vol. 54, no. 1, pp. 19–45, 2012.

[47] A. M. Abd-Alla and S. M. Abo-Dahab, "Magnetic field and rotation effects on peristaltic transport of a Jeffrey fluid in an asymmetric channel," *J. Magn. Magn. Mater.*, vol. 374, pp. 680–689, 2015.

[48] S. Srinivas, R. Gayathri, and M. Kothandapani, "Mixed convective heat and mass transfer in an asymmetric channel with peristalsis," *Commun. Nonlinear Sci. Numer. Simul.*, vol. 16, no. 4, pp. 1845–1862, 2011.

[49] Y. Wang, T. Hayat, N. Ali, and M. Oberlack, "Magnetohydrodynamic peristaltic motion of a Sisko fluid in a symmetric or asymmetric channel," *Physica A: Stat. Mech. Appl.*, vol. 387, no. 2-3, pp. 347–362, 2008.

[50] A. M. Abd-Alla, E. N. Thabet, and F. S. Bayones, "Numerical solution for MHD peristaltic transport in an inclined nanofluid symmetric channel with porous medium," *Sci. Rep.*, vol. 12, no. 1, p. 3348, 2022.

[51] E. Elshehawey, A. E.-R. El-Saman, M. El-Shahed, and M. Dagher, "Peristaltic transport of a compressible viscous liquid through a tapered pore," *Appl. Math. Comput.*, vol. 169, no. 1, pp. 526–543, 2005.

[52] Z. Asghar, K. Javid, M. Waqas, A. Ghaffari, and W. A. Khan, "Cilia-driven fluid flow in a curved channel: effects of complex wave and porous medium," *Fluid Dyn. Res.*, vol. 52, no. 1, p. 015514, 2020.

[53] R. W. Fox, A. T. McDonald, and P. J. Pritchard, "Introduction to Fluid Mechanics", 8th ed. Hoboken, NJ: Wiley, 2011.

[54] B. R. Munson, D. F. Young, and T. H. Okiishi, “Fundamentals of Fluid Mechanics”, 7th ed. Hoboken, NJ: Wiley, 2013.

[55] A. Abbasi, S. U. Khan, W. Farooq, F. M. Mughal, M. I. Khan, B. C. Prasannakumara, ... and A. M. Galal, “Peristaltic flow of chemically reactive Ellis fluid through an asymmetric channel: Heat and mass transfer analysis,” *Ain Shams Eng. J.*, vol. 14, no. 1, pp. 101832, 2023.